# COHERENT DIFFRACTION IMAGING (CDI)

*Investigating Problems with Phase Reconstruction*

Bryony D Brown

Submission date: 26th of March 2013
Project Supervisor: Professor Ian Robinson
Secondary supervisor: Dr Jesse Clark

Abstract - This paper investigates how the algorithms used in CDI work for 2D objects and how adding different phase structures effects the programs ability to reconstruct good images. The program was not able to reconstruct objects with strong phase variation which biases the results for particular phase structures unless extra real space information was included in the constraint process.

| | Page Number |
|---|---|
| **Table of acronyms/ abbreviations** | **2** |
| **1 Introduction** | **3** |
| 1.1 What is CDI? | **3** |
| 1.2 Aim of the project | **3** |
| **2 Method** | **3** |
| 2.1 Program construction | **3** |
| 2.2 ER- algorithm | **4** |
| 2.3 HIO- algorithm | **5** |
| 2.4 Settings of the program | **5** |
| 2.4.1 Sample space constraint | **5** |
| 2.4.2 Number of Iterations | **6** |
| 2.5 Data creation | **6** |
| 2.6 Problems occurred | **7** |
| 2.7 Creating objects with phase | **8** |
| **3 Results** | **9** |
| 3.1 Effect of object shape | **9** |
| 3.1.1 Square/Diamond | **9** |
| 3.1.2 Rectangle | **9** |
| 3.1.3 Circle | **10** |
| 3.2 Effect of phase - Linear | **11** |
| 3.3 Effect of phase - Quadratic | **14** |
| 3.4 Effect of phase - Quadratic shifted | **15** |
| 3.5 Effect of phase - Saddle point | **17** |
| 3.6 Effect of phase - Saddle point shifted | **20** |
| **4 Improvements** | **25** |
| 4.1 Including magnitude information | **25** |
| 4.2 Including phase information | **26** |
| **5 Conclusion** | **26** |
| **6 References** | **27** |
| **7 Appendix** | **29** |
| 7.1 ER Programing | **29** |
| 7.2 HIO Programming | **30** |
| 7.3 Phase structure program | **31** |

| **Abbreviation / acronym** | | Comments |
|---|---|---|
| CDI | Coherent diffraction Imaging | |
| 2D or 3D | 2 dimensional or 3 dimensional | Reference to number of proportions |
| DFT | Discrete Fourier transformation | |
| FFT | Fast Fourier transformation | |
| IDFT/IFFT | Inverse Fourier transformation | |
| ER | Error reduction | Type of algorithm |
| HIO | Hybrid input output | Type of algorithm |
| Ne-9 | $Nx10^{-9}$ | N represents a number |
| | | |
| | | |
| | | |
| | | |

# 1. Introduction

## 1.1 What is CDI?

Coherent diffraction imaging (CDI) is the recovery process of an object's image from its diffraction pattern by computational phasing (Clark, 2012). As no lenses are used, there is the potential of the resolution of the images only being limited by the wavelength of the beam, exposure time and aperture size. The method is set up using a coherent wave source, this is usually high energy x-rays in which case the process is called x-ray CDI. Coherency is very important, as the waves need to have fixed phase relative to one another in order for the interference to produce a useable diffraction pattern. If the relative phases were allowed to differ the diffraction pattern would alter with time and the pattern would become blurred and unusable. After the diffraction of the waves through the object the pattern is collected by a detector that collects the data as counts of the number of photons or electrons hitting each pixel. The diffraction pattern corresponds to the magnitude information of the object in reciprocal (sometimes called Fourier) space but the detector cannot collect phase information about the wave front. In order to recreate the image of an object both the phase and magnitude information is needed so an iterative reconstruction programme can be used to recreate the phase information and therefore reconstruct the object. The ability of the program to reconstruct the phase is also a limiting factor in the image quality and resolution as it is the replacement of the lens (Robinson, 2009).

## 1.2 Aims of the project

The overall aim of the project was to investigate how the algorithms used in CDI work. This was done in a two-step process: building a reconstruction program that reconstructs 2 dimensional (2D) shapes and to investigate how the program results are affected by adding different phase structures across the object.

# 2. Method

## 2.1 Program construction

Building the program was done in two stages as it was based on a format that uses two algorithms in combination: Error Reduction (ER) and Hybrid Input Output (HIO) algorithms. Figure 1 shows a schematic of the overall picture of how the algorithms were run separately but used in combination

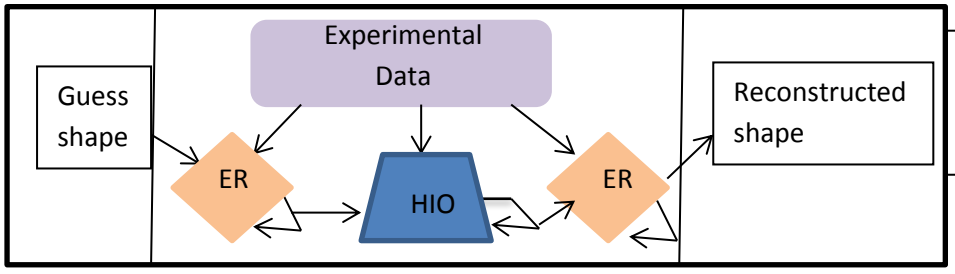


***Figure 1*** - A schematic of how the algorithms are used in combination

to produce the reconstruction. Each of the algorithms can be used separately to retrieve the phase

information as explained in sections 2.2 and 2.3. The HIO algorithm is much stronger and has less of problems encountered by the ER algorithm although only reaches its full potential when it is combined with ER (Minkevich, 2012). The number of cycles of each algorithm was optimised before investigation into the reconstruction process was carried out and is discussed in section 2.4.

2.2 ER - Algorithm

The ER algorithm (Fienup, 1982) is a fast iterative algorithm and uses alternating constraints on a

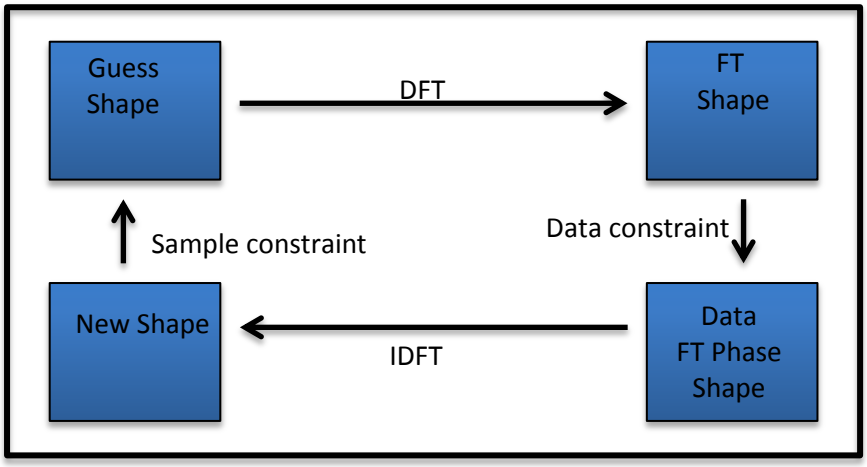


***Figure 2*** – Illustration of the ER algorithm

trail solution in real and reciprocal space. Figure 2 is an illustration of how the algorithm is programmed. At first a trial solution is formed labelled here as the guess shape. This is then Discrete Fourier Transformed (DFT) into reciprocal space. What is formed is labelled at the Fourier transform (FT) shape. A data constraint is applied in reciprocal space. This is the known magnitude information diffraction pattern collected experimentally and is combined with the trial solutions phase information. After the data constraint is applied the information is then inverse discrete Fourier transformed (IDFT) back into real space. The last step before the next iteration cycle is to apply a sample constraint. This assumes that the dimensions of the shape or object are known so solutions outside of the dimensions are set to zero and the solutions within the object are kept to form the new trial solution. The data constraint represents a non-unique projection operator; if this was the only constraint applied the reconstruction could converge on any number of possible solutions and not the wave phase at the object surface (Bauschke, 2002). The sample constraint drives the algorithm towards the wave phase at the object solution because this is the only solution that has the sharp defined edges of the shape dimensions. The ER algorithm is known as a local minimizer algorithm (Fienup, 1982) as it reduces the error from the previous solution. Reconstructing the phase of objects often involves many different local minimums, so depending on the starting trial solution or guessed object magnitude and phase it's very easy for the ER algorithm to get stuck in a local minima rather than the overall minimum (Köhl, 2012). This means that only using ER the program may not converge on the correct solution. Another problem with using the ER algorithm alone is stagnation, it may take many iterations for the error to be reduced and then a larger number of iterations are needed to verify if the program is stuck in a local minimum or stagnating. This increases the program run time and computer power needed. HIO is one of many algorithms that were created in order to deal with the stagnation and local minima problem of ER. For the ER algorithm coding please see the appendix section 7.1.

2.3 HIO – Algorithm

Fienup proposed the HIO algorithm in the paper 'phase-retrieval stagnation problems and solutions' in 1986(Fienup, 1986). It uses the same basic iteration process as ER except for a slight difference in the sample space stage constraint. As with the sample space constraint in ER the solutions inside the dimensions of the object are kept. However unlike the sample constraint in ER the solutions outside of the dimensions are also allowed to vary and are not set to zero. This works by subtracting the previous iteration output multiplied by a real parameter from the current iteration output, all done in the frame outside of the object dimensions. This forms a sort of weighted average between the previous iteration and the current iteration with the real parameter, often known as β, within the typical range of 0.5 to 1.0 (Köhl, 2012& Fienup, 1986). Starting with random trial solutions or guess shapes HIO consistently reconstructs the same structure and so it is considered a reliable algorithm (Williams, 2007). The solutions being allowed to vary outside of the sample constraint makes this more powerful than ER as it is much better at avoiding both stagnation and local minima. However because its weighted average technique it can only reach its full potential when used in combination with ER as the error is never allowed to reach a minimum in HIO alone. The format of $N_{ER}$ cycles of ER followed by $N_{HIO}$ cycles of HIO and then $N_{2ER}$ cycles of ER again, as shown in figure 1, was used as this was found to have the least amount of stagnation. For the programming script of the HIO algorithm please see the appendix section 7.2.

2.4 Program Settings

The 2009 version of Matlab (Matlab 7.8.0 (R2009a)) was used to write the program when producing figures and images several settings had to be optimised in order to see the results clearly. A colour bar was added to show the different phase and magnitude gradients. The different images of the matrices were also zoomed so that the phase and structure of the objects could be seen clearly. A title was given to the images and axis numbering the rows and columns of the matrices was also included.

2.4.1 Sample Space Constraint

A short investigation into the sample space constraint was done to see how close to the object dimensions the sample space constraint needed to be for the program to successfully reconstruct the object. This was done using a simple square of magnitude one and zero phase. To measure the error of the reconstruction the $\chi^2$ value was calculated comparing the experimental data diffraction pattern with the reconstructed shape FT magnitude information. With the sample constraint set at the dimensions of the object both HIO and ER reproduced the exact image within one or two iterations. Increasing the sample space constraint by one pixel larger than the object requires around 1000 iterations of ER to reproduce the object with a $\chi^2$ error of just over 2e-9. HIO requires around 100 iterations (with less than 10 iteration of ER to remove solutions outside of the sample space) to produce a $\chi^2$ error of just over 7e-9. Increasing the number of HIO iterations to the same amount of ER reduces the $\chi^2$ error down to around 2e-12. The result of the number of iterations and the error produced is summarised in Table 1. For ER you can clearly see that a sample space larger than one or two pixels above the shape dimensions requires a much larger number of iterations to produce results with similar errors. These results are consistent with previous results found for early phasing algorithms which concluded that several thousand iterations were needed to reconstruct

reliable results (Vartanyants, 1997). The run time for 100000 iterations of ER took around 100 seconds. This is a considerable run time and was not practical for investigating the phase as multiple runs of the program for different shapes and phases was intended to be carried out. This is also a clear demonstration of the stagnation problems of ER for larger sample constraints. At around 5 pixels larger the reconstruction began to totally break down and the shape became unrecognisable. HIO was a much faster only requiring a maximum of 1000 iteration to produce errors lower than ER for all the sample constraint sizes. This is again consistent with algorithm reliability measurements. In Williams 2007 paper: Effectiveness of iterative algorithms in recovering phase in the presence of noise, found that as few as 50 iterations of HIO were needed to reproduce consistent reliable results (Williams, 2007). Recognisable shapes were reproduced to sample constraints up to 5 pixels. Results above 5 pixels to 9 pixels did produce reasonable errors and reconstructions but the iterations need to be increased from 1000 to 10000 or 100000 massively increasing the run time and so these were not included as running the program enough times to verify the error would have taken a considerable amount of time. Above 9 pixels the HIO reconstruction also became unrecognisable.

**Table 1 - A table showing the errors associated with sample space sizing**

| **Sample Space Constraint** | **ER** | | **HIO** | |
|---|---|---|---|---|
| | **Iterations** | **$\chi^2$ Error** | **Iterations** | **$\chi^2$ Error** |
| **1 Pixel Increase** | 1000 | 2e-9 | 100 | 7e-09 |
| | | | 1000 | 2e-12 |
| **2 Pixel Increase** | 1000 | 5.5e-8 | 1000 | 1e-12 |
| | 100000 | 9e-9 | | |
| **3 Pixel Increase** | 100000 | 3e-8 | 1000 | 9e-11 |
| **4 Pixel Increase** | 100000 | 1.5e-8 | 1000 | 8e-11 |
| **5 Pixel Increase** | 100000 | 2e-7 | 1000 | 2e-10 |

For the investigation a sample space size of one pixel larger than the shape dimensions was chosen and used throughout. This was so that the run time and number of iterations could be kept low as well as to represent the systematic error in object dimension measurement.

2.4.2 Number of Iterations

Using data from the sample space investigation as well as short investigation into iteration number combinations the programme used 10 iterations of ER followed by 100 iterations of HIO and then 500 iterations of ER again. This was found to have a suitable short run time and produced reliable results for both the errors and reconstructed shapes.

2.5 Data Set Creation

When experimentally compiling results several factors need to be taken into account. The coherency of the propagating beam has already previously been mentioned and this is discussed further in Clark's 2012 paper: High- resolution three-dimensional partially coherent diffraction imaging (Clark, 2012). The object size is required to be small. This is due to the condition that the sample needs to be totally illuminated by the propagating wave; the transverse length of the wave must exceed the object dimensions. This allows for scattering from all parts of the sample contributing to the diffraction pattern (Robinson, 2009). The detector distance and sampling condition are also factors

that play an important role in the collection of the data. The detector must be positioned so that it can resolve the finest fringes, the detection of which requires a minimum of two detector pixel spacing's per fringe (Miao, 2000). This is the minimum requirement for the 'oversampling' condition which is defined as the Nyquist rate; twice the highest frequency contained within the signal.

As this is a computational investigation, no real experimental data was used instead, the 'data' was computed. A 128 by 128 matrix was used with each cell of the matrix representing one pixel. A small object, sized at 10 by 10, and centred in the matrix was then programmed. This can be seen in Figure 4. The shape was pre-set to have a magnitude of one in all pixels for all calculations the phase was kept at 0 for the program construction but was later varied for the investigation. This was then Fast Fourier transformed (FFT) into reciprocal space to produce the data diffraction pattern. This can be seen in figure 3.

***Figure 3*** Computed version of an experimental diffraction pattern. The axis numbers represent the column and row numbers of the matrix. The colours represent the density of electrons or photos that hit that pixel.

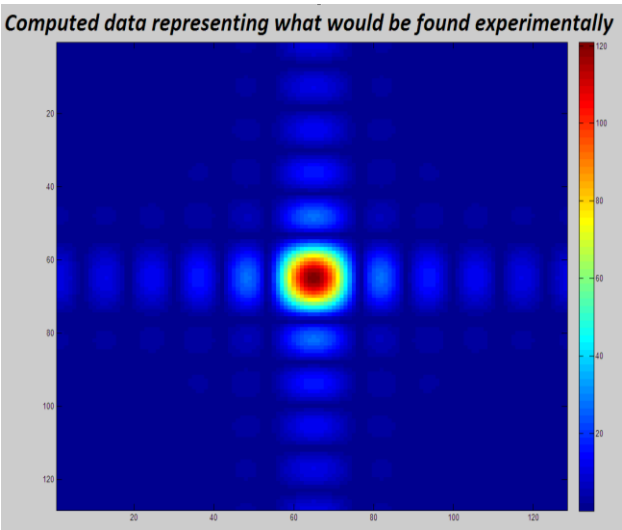


***Figure 4*** The object representation in real space. Images of the reconstructions will be zoomed in to clearly show the structure of the reconstruction. You can see the object is very small compared to the size of the matrix and has an even magnitude of 1 within the shape; there is zero magnitude outside of the shape

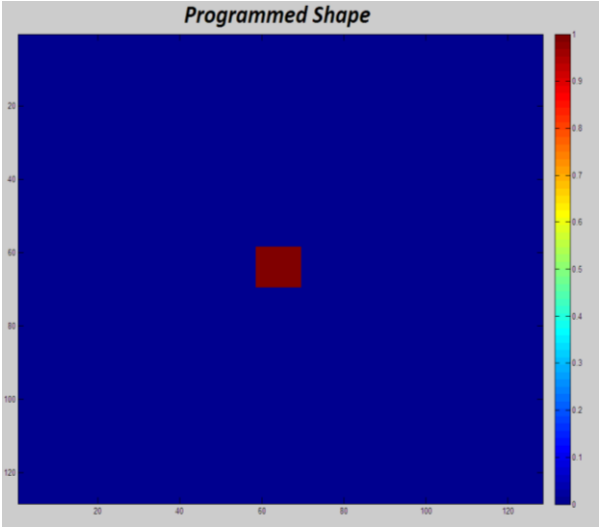


2.6 Initial problems

The spacing between fringes is directly related to the object size; many techniques estimate the dimensions of the sample constraint from the fringe spacing and allow the support to evolve on successive cycles (Marchesini, 2003). This posed problems for sizing the object comparatively to the matrix size. The larger the object was sized in the matrix the smaller the diffraction pattern became. At around 20 pixels in width and height the objects diffraction pattern fringes were no longer recognisable and so the over sampling condition was no longer being met. This meant the reconstruction broke down and would not produce recognisable results. In order to avoid this

problem the shape sizes were kept small to around 10 pixels in diameter and zooming of the images was done with the zoom program in Matlab rather than just enlargements of the objects.

2.7 Creating Phase

For most of the program construction the object was programed to have a zero phase structure. The second part of the investigation started to look at how the phase of objects affects the reconstruction process. Numerically the phase can be represented by equation 1.

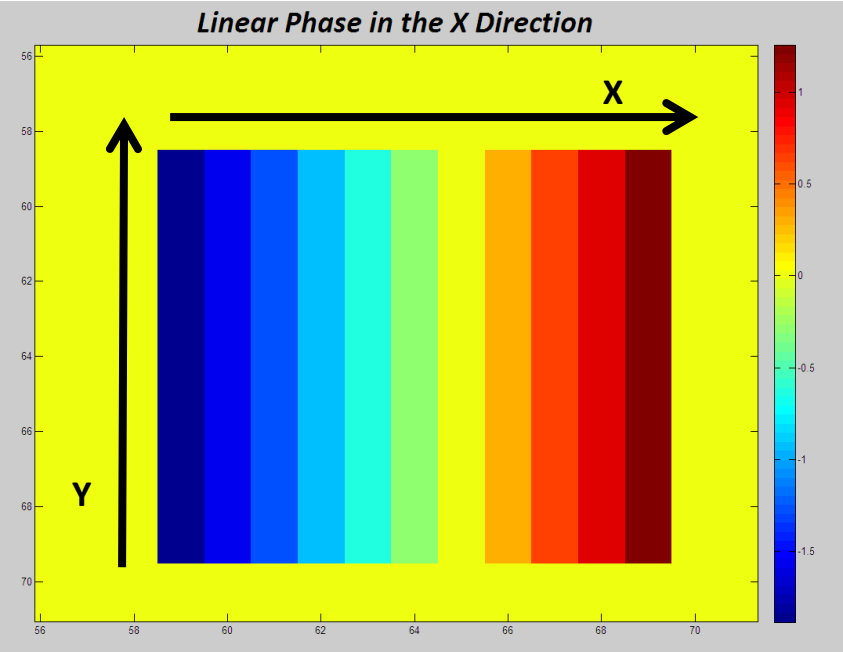


***Figure 5*** - An example of the phase directions this linear phase has the equation (2): phase=2π*X*c where c is a constant in this case it takes the value of 0.05. Outside of the object the phase is 0 represented here as yellow.

Equation (1): f(**x**) =exp (iφ(**x**)) * Sample constraint) (Köhl, 2012)

Where i is the imagery number and φ(**x**) represents the phase equation. The sample constraint allows the phase to vary only within the object dimensions, outside of which the phase is 0. In order to do this the object matrix needed to be transformed into a mesh grid so that individual rows, columns and cells of the matrix could be accessed and programmed. The mesh grid was programmed so that the columns of matrix represented the Y direction and the rows of the matrix represent the X direction. Figure 5 shows a square object with linear phase in the x direction.

Linear phase was then extended to form more complex linear structures such as figure 6, quadratic phase structures of objects, as well as saddle points and a combination of structures and its effect on the reconstruction was also studied. Please refer to the results section for images of these structures and appendix section 7.3 for phase structure programming.

***Figure 6*** - The blue line representing the phase direction. This phase structure has the equation
(3): 2π*X*c - 2π*Y*d
Where both c and d are constants

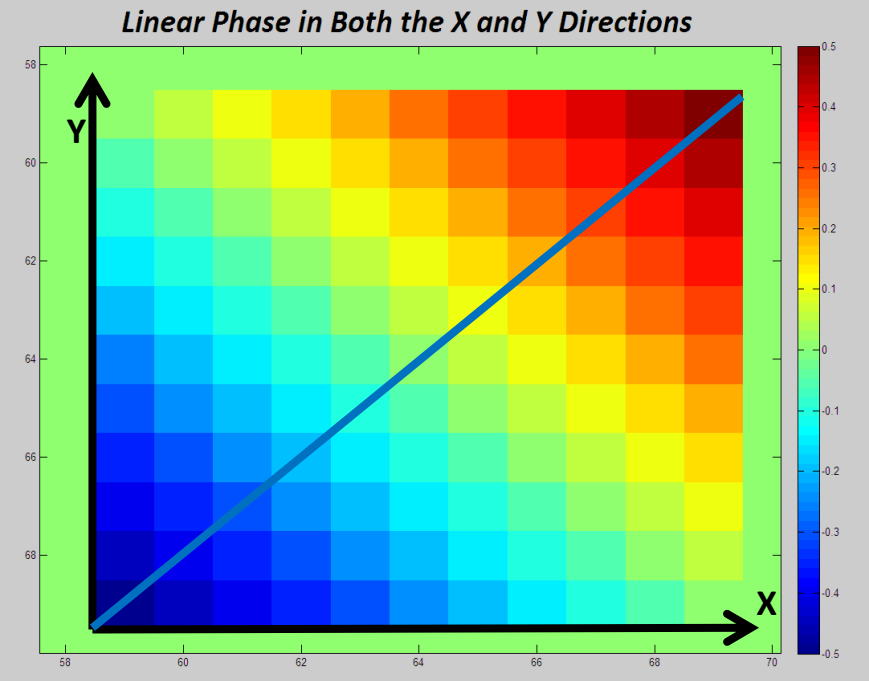


## 3. Results

3.1 Effect of object shape

The shape of small objects is often deformed when using high energy processes to image them (Cha, 2010). This affects their diffraction pattern and so ultimately will affect the reconstruction of the image of the object. A short investigation into how the object shape affects the diffraction pattern and overall reconstruction was done to decide upon a suitable shape to continue the investigation with as well as to gain an insight into how the diffraction patterns change with shape.

3.1.1 Square/ diamond

Figures 3 4 5 and 6 show the square shape that was used throughout the initial programming. Rotating the square to form a diamond shape resulted in a rotation of the diffraction pattern by 45° (or the amount the square was rotated by).

3.1.2 Rectangle

Stretching the square in the Y direction to form a rectangle resulted in the diffraction pattern being stretched in the X direction see figures 7 and 8 for examples of this. Stretching the square in the X direction to form a rectangle resulted in the diffraction pattern being stretched in the Y direction. These results have also been found in previous studies such as w. Cha article on Exploration of crystal stains using coherent x-ray diffraction. (Cha, 2010). The Diffraction pattern shows a high intensity rectangular shape in the middle the fringes also look rectangular and have been elongated in the x direction. The diffraction pattern stretches in the opposite dimension to the object stretch.

***Figure 7***- The diffraction pattern of a rectangle with the larger dimension in the Y direction.

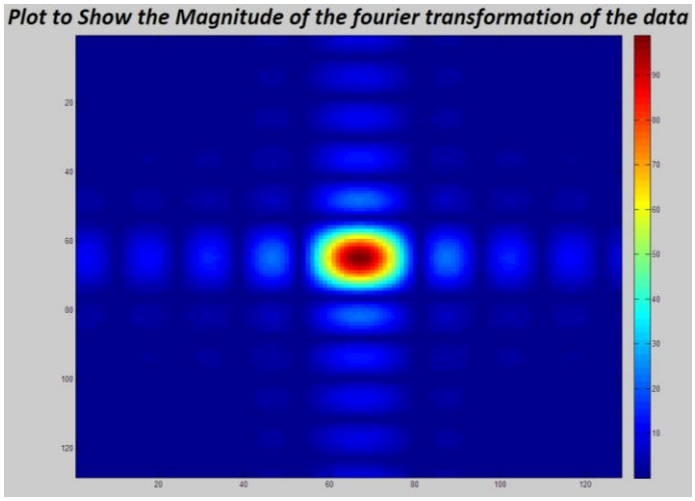


***Figure 8*** - Rectangular Object - Y stretch

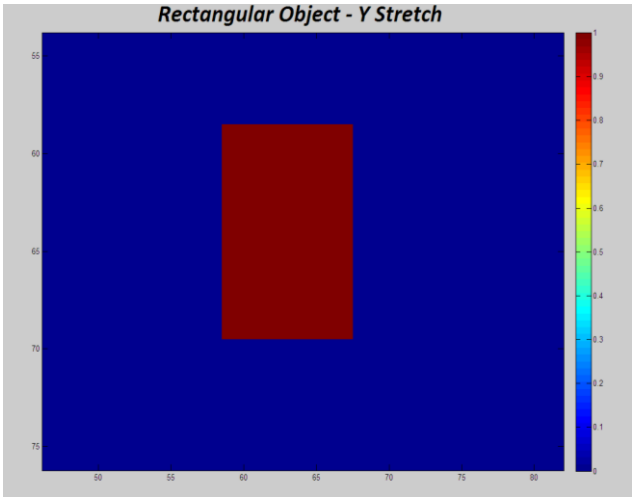


3.1.3 Circle

As well as changing the shape the sample constraints could also be altered or left as a square of the correct dimensions. Both of these worked well for the diamond and rectangle reconstructions but the circle reconstruction using a square sample constraint didn't reconstruct as well as the circle sample constraint. Figure 9 shows the programmed object, figure 10 shows the circles diffraction pattern, figure 11 shows the reconstruction using a circle sample constraint one pixel larger than the object and figure 12 shows the reconstruction using a square sample space.

***Figure 9*** – Circular Object the magnitude is 1 in every pixel and has a phase of 0.

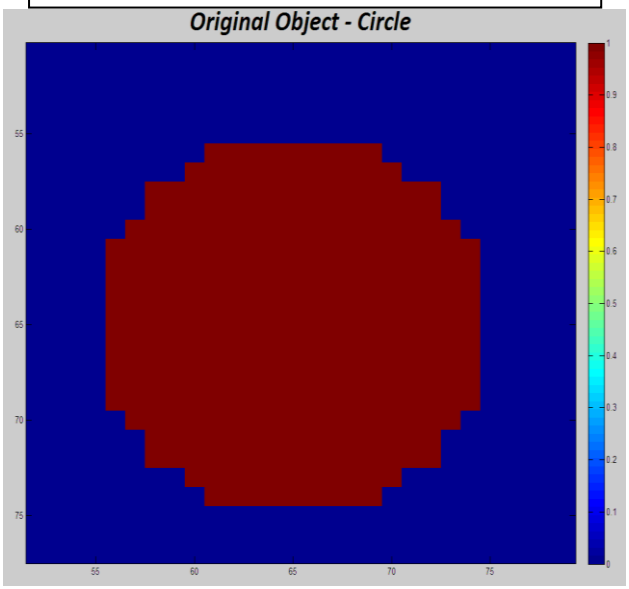


***Figure 10*** – Diffraction Pattern of a circle.

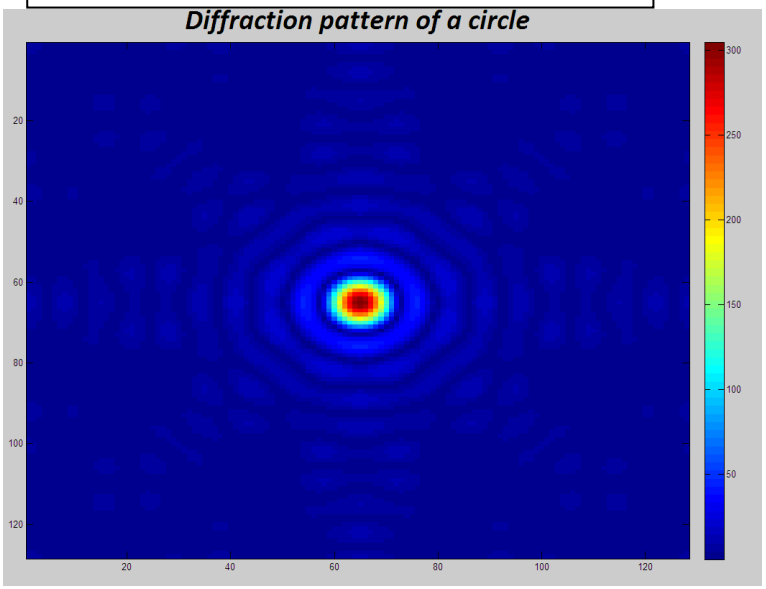

***Figure 11*** – The reconstruction using a circular sample constraint one pixel larger than the object $\chi^2$ error 2e-12. The circle represents the position and size of the circular sample constraint.

***Figure 12*** – The reconstruction using a square sample constraint the $\chi^2$ error has now grown to around 7e-008. The black square represents the size and position of the square sample constraint.

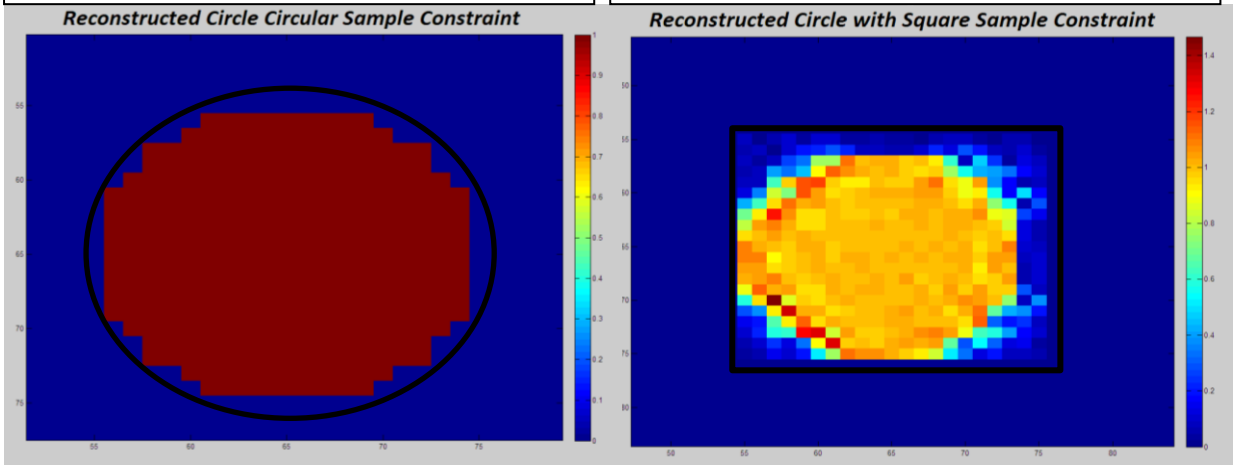


The circle diffraction pattern looks very different from the square and rectangle, the centre again shows a high density but it is circular rather than square or rectangular. The fringes are also circular and the first few encompass the entire central section before becoming split and tapering off.

Comparing the circular and the square sample constraint you can clearly see that the square sample constraint was much less effective than the circular constraint. This was a different result from the previous objects and it is most probably due to the circle having a 4 or 5 pixel gap between the sample constraint edge and the object edge at some points. This could allow for large local minima around the overall minimum and so the reconstruction takes longer to find the correct solution.

After programing several different shapes the square was chosen to be the main shape analysed because it required the simplest programming and had the shortest run time. It was assumed that when phase was introduced the number of iterations needed to gather results would need to be increased to optimise the results and so the shape with the shortest run time was the most preferable.

3.2 Effect of phase – Linear

The process of adding linear phase (also known as a phase ramp) across the object has previously been described in section 2.7.

***Figure 18*** – The reconstruction of the Square with a small phase ramp.

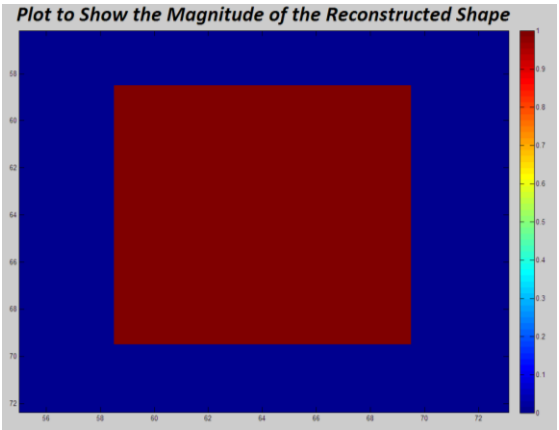

The expected result was that a linear structure corresponds to a translation of the diffraction pattern in the direction of the phase. First relatively low phase values were programmed with phases less than 2π being used. Figures 18- 22 were all programmed with: Phase=2πXc the constant c had the value 0.05.

***Figure 19*** – The diffraction pattern for a square with a small phase ramp.

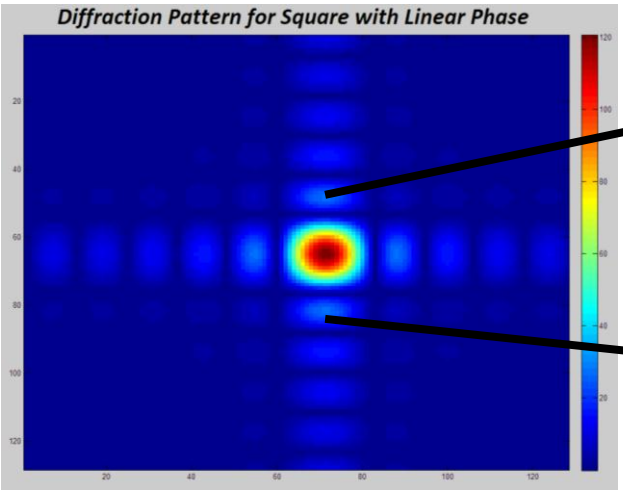


***Figure 20*** – Zoomed version of figure 19 to show that diffraction pattern is no longer in the centre.

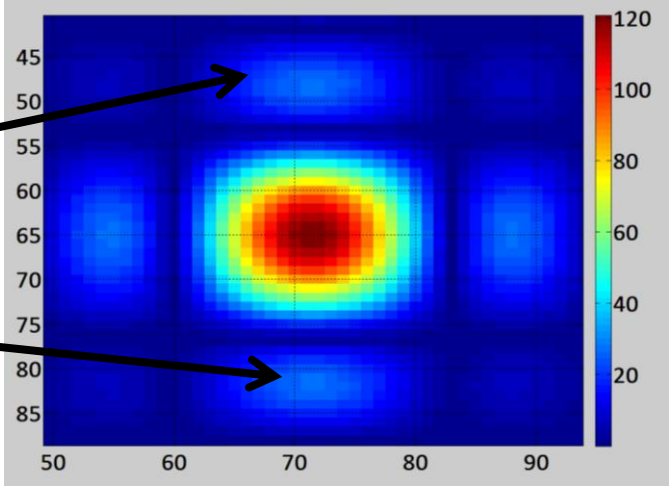


For phase values less than 2π the program could easily reconstruct both the phase and magnitude of the shape as shown by figures 22 showing the phase and figure 18 showing the magnitude. Figure 19 shows the diffraction pattern of this shape and by zooming in on the central section of the matrix as done in figure 20 you can clearly see that the centre of the diffraction pattern has shifted to around 72 rather than being at the centre of the matrix pixel 64. See appendix section 7.3 for linear phase structure.

Increasing the phase ramp above values of 2π the reconstruction program encountered problems. A recognisable shape of magnitude one was no longer reconstructed even with a tight support constraint and the diffraction pattern now appeared to be heavily shifted.

***Figure 24*** – The diffraction pattern for strong linear phase.

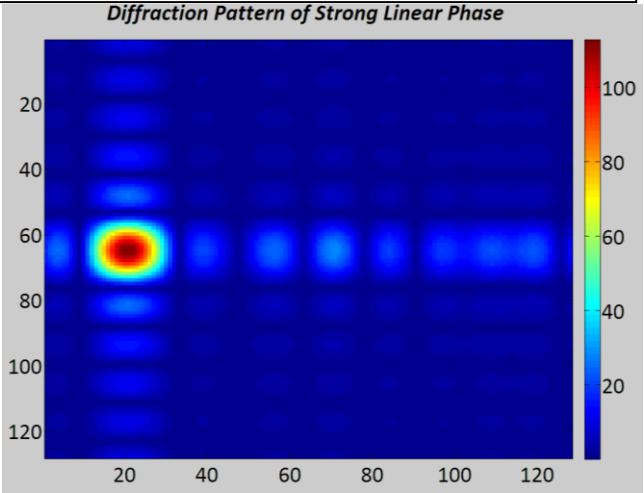


***Figure 25*** – The Magnitude of the reconstructed shape.

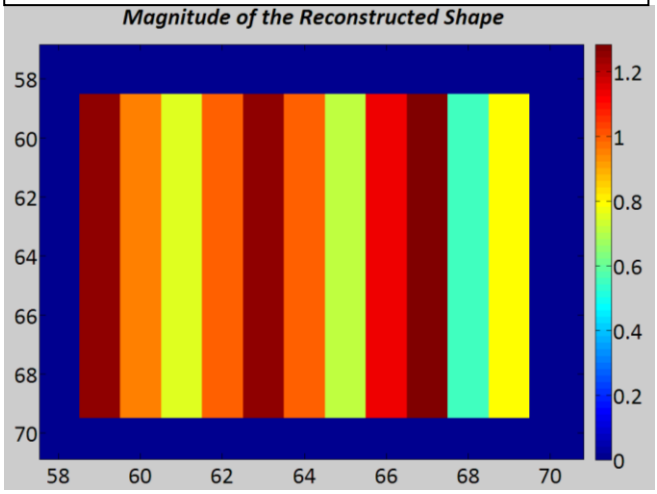


***Figure 26*** - The linear phase of the original shape. This phase contains around 4 phase wraps. The colour bar scale is common to both figure 26 and figure 27.

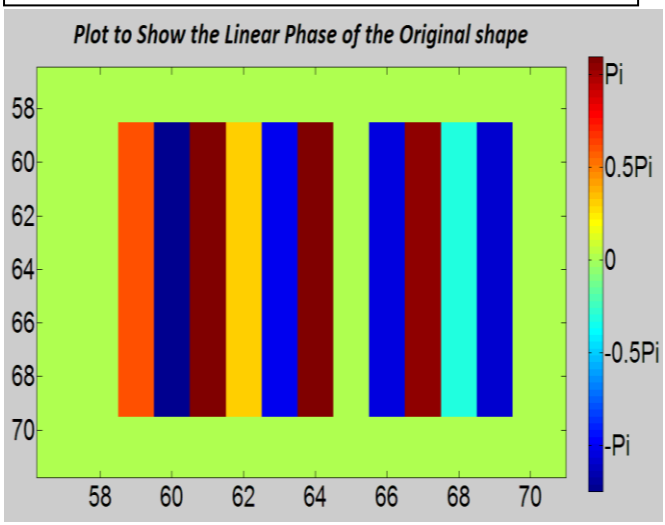


***Figure 27*** - The linear phase of the reconstructed shape. This phase also contains around 4 phase wraps. The colour bar scale is the same for both Figures.

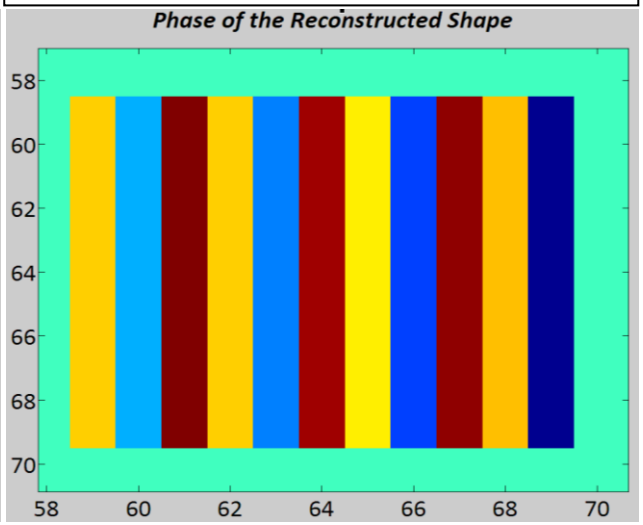


The Reconstruction has had clear problems with reconstructing the original shape. Although the phase has 4 wraps (a phase wrap is defined as a change through 2π in this case it is from –π to +π) in both the original shape and reconstruction the magnitude of the reconstruction has become stripy and alters from 1.2 down to 0.5. As the linear phase ramp corresponds to the shape being translated in the direction of the phase relative to the propagating beam, by shifting the diffraction pattern back into the centre the program is able to successfully reconstruct the object magnitude.

Phase structure close to or over 2π is often referred to as strong phase. Objects with strong phase have what is known as a non- uniqueness problem. The non- uniqueness can occur for multiple reasons some of which are discussed later, but one of the most important is a result of the

propagating diffracted wave. This is referred to as the propagation uniqueness problem which is that the wave front of the object has the same magnitude diffraction pattern as the wave front after it has travelled or propagated a short distance d. This means that the Fourier transformation of the diffraction pattern is non- unique and leads to multiple solutions linked by propagation. For Weak phase variation across structures the sample space constraint selects a focal plane which brakes the non uniqueness but this is no longer applicable for strong phase variation (Huang, 2011).

3.3 Effect of phase – Quadratic

For quadratic phase, two phase structure have identical diffraction patterns; phase = $c1X^2$ +c2Y and Phase = c2Y –$c1X^2$ where c1 and c2 are both constants. Examples of these phase structures are shown in Figures 28 and 29.

***Figure 28*** - Quadratic Phase = $c1X^2$ + c2Y The scale is common to figure 28 and 29.

***Figure 29*** - Quadratic Phase = c2Y - $c1X^2$ The scale is common to figure 28 and 29.

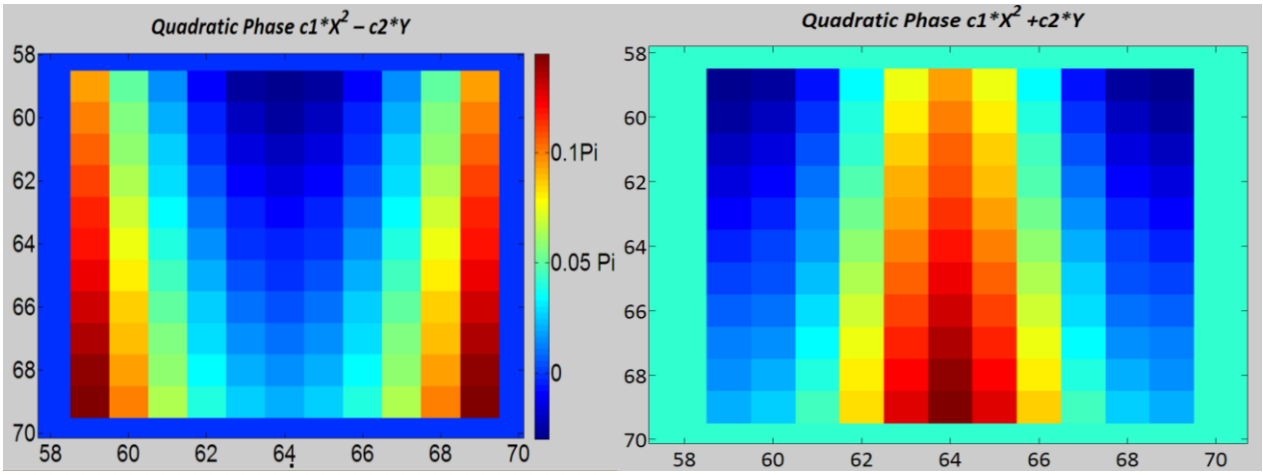


As it is not possible to distinguish which phase structure is the correct from the diffraction pattern the expected result is that each phase structure is reconstructed 50% of the time. A low π phase

***Figure 30*** – The diffraction pattern for the quadratic phase with low phase variation.

***Figure 31*** – The reconstructed shape for low phase variation.

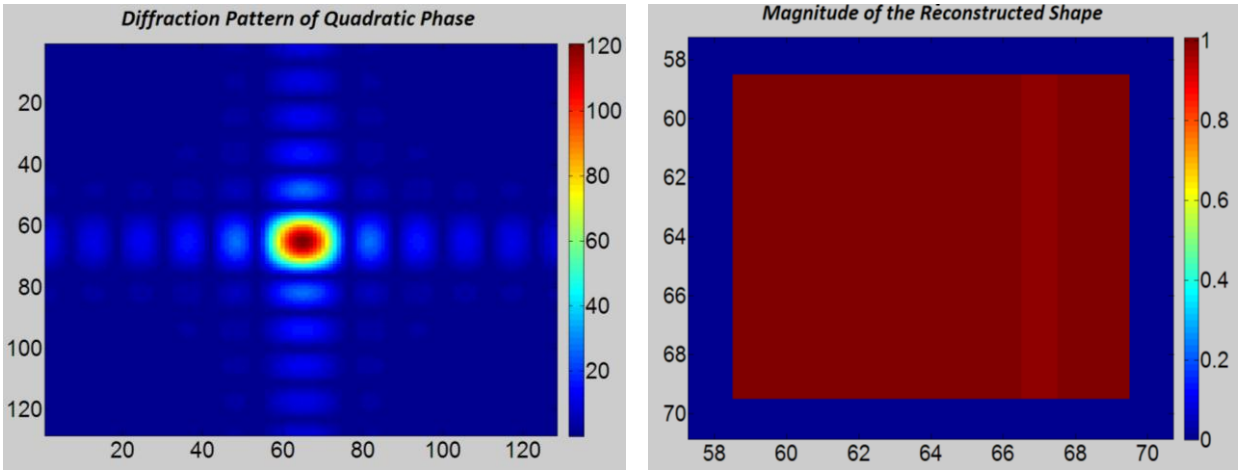

variation is used because for the quadratic phase structure the phase propagation issue is more prevalent because of fringe mixing as shown in figure 32. For low π phase variation the fringes are still clearly defined as shown in figure 30. Figure 31 shows an average reconstruction of the shape. The magnitude is mostly correct with one or sometimes two slight faults. The $\chi^2$error for this reconstruction was very good normally a figure around 2e-12 for this low phase variation.

As expected, each phase structure was recreated 50% of the time each for around 100 runs of the reconstruction. Increasing the phase variation to vary across the object by around half π caused the fringes in the diffraction pattern to no longer be distinguished limiting the reconstruction to a range of possibilities due to the propagation uniqueness problem discussed earlier (Huang, 2011).

***Figure 32*** – The diffraction pattern of the stronger phase quadratic.

***Figure 33*** – A zoomed version of figure 32 to show the fringes boundaries have become difficult to define

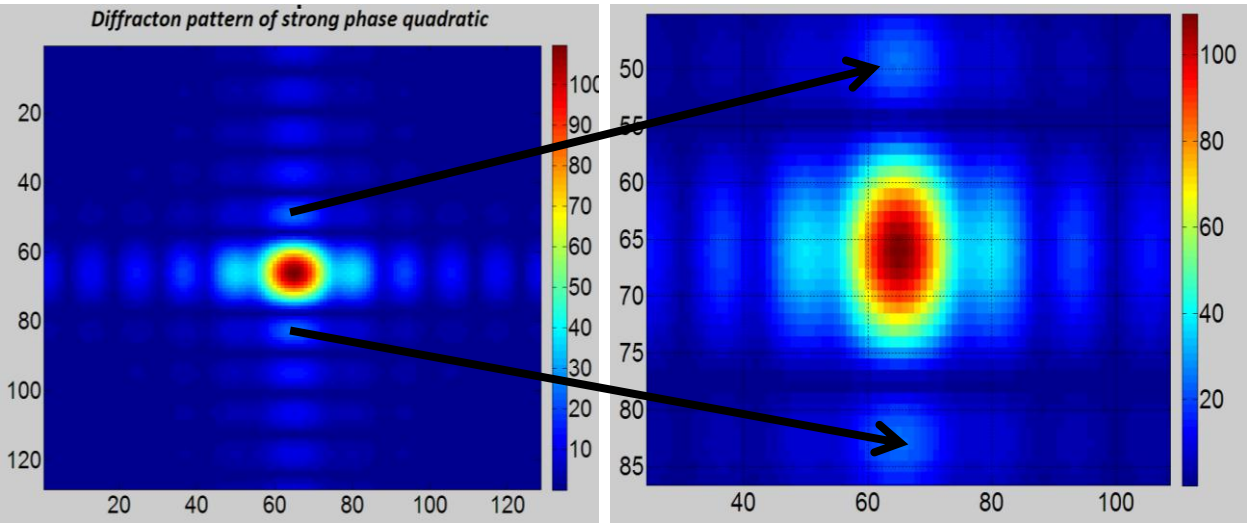


The stronger phase quadratic the reconstruction has again broken down like for the linear strong phase. Unlike the linear the diffraction pattern has not been shifted and so the shifting technique cannot be used here. The reconstructed shape has a stripy magnitude structure varying from 1.6 down to 0.6. The phase reconstruction has a linear structure in the Y direction which varies from 0.8Pi down to -0.6Pi a much smaller range than the phase structure of the object.

3.4 Effect of phase – Quadratic shifted

Adding a shift to the quadratic as shown in figure 37 had several effects on the reconstruction. The $\chi^2$ error was reduced so that the shape reconstruction was much closer to the original object. It had the same effect as reducing the phase strength so stronger phase objects could be programmed. Figures 36 to 39 have been programed with a phase variation of just over 0.5π as lower π variation had very subtle structures that were more difficult to see but of the same structure as figure 38 and 39. Like for a linear shift the centre of the diffraction pattern was shifted but in the Y direction rather than the X direction (the direction the phase was shifted). The last effect was the number of times the reconstructed phases were now produced. Figure 38 the opposite phase structure to the objects phase was reproduce 75% of the occasions where as Figure 39 the phase structure closest to the

original object was only reconstructed on 25% of the occasions. This was for around 200 reconstructions.

On reversing the phase structure to the opposite sign with a one pixel phase shift again the phase of the opposite nature to the objects was reproduced on 75% of the occasions with the same phase structure whereas the closest phase structure was only reproduced on 25% of the occasions (again for around 200 reconstructions). Shifting the phase structure by two pixels reconstructed the two expected phase structures with two pixel shifts but on this occasion the most similar phase structure was reproduced on 75% of the occasions with the opposite phase structure being reproduced only

***Figure 34*** – The reconstructed object of the strong phase quadratic

***Figure 35*** – The reconstructed phase of the strong phase object

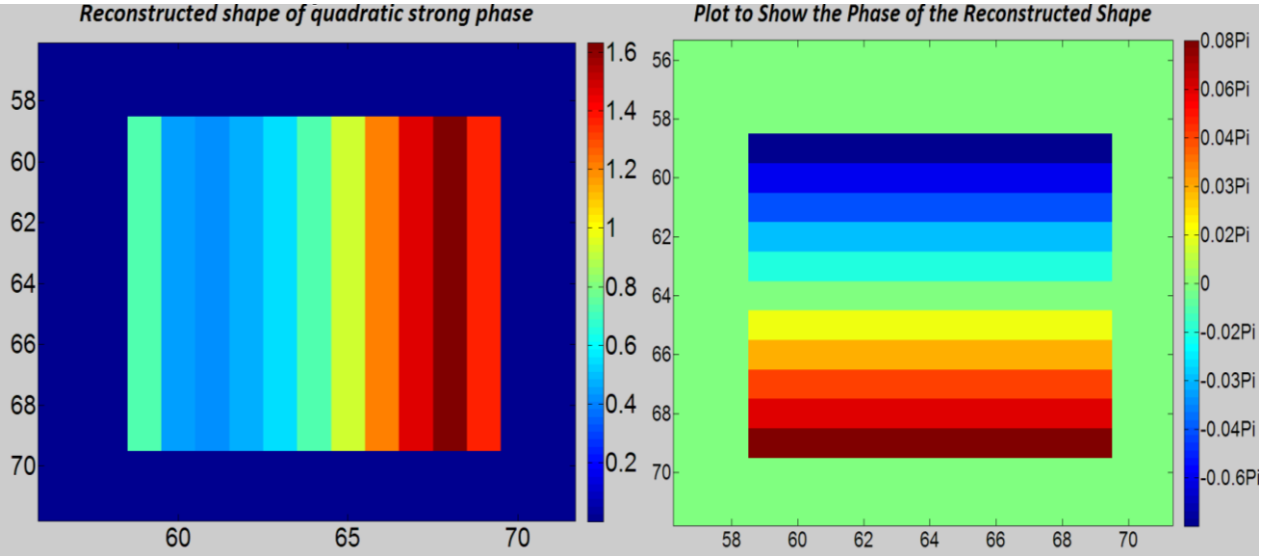


***Figure 36*** – The reconstructed object for the shifted quadratic phase.

***Figure 37*** – The reconstructed object for the shifted quadratic phase.

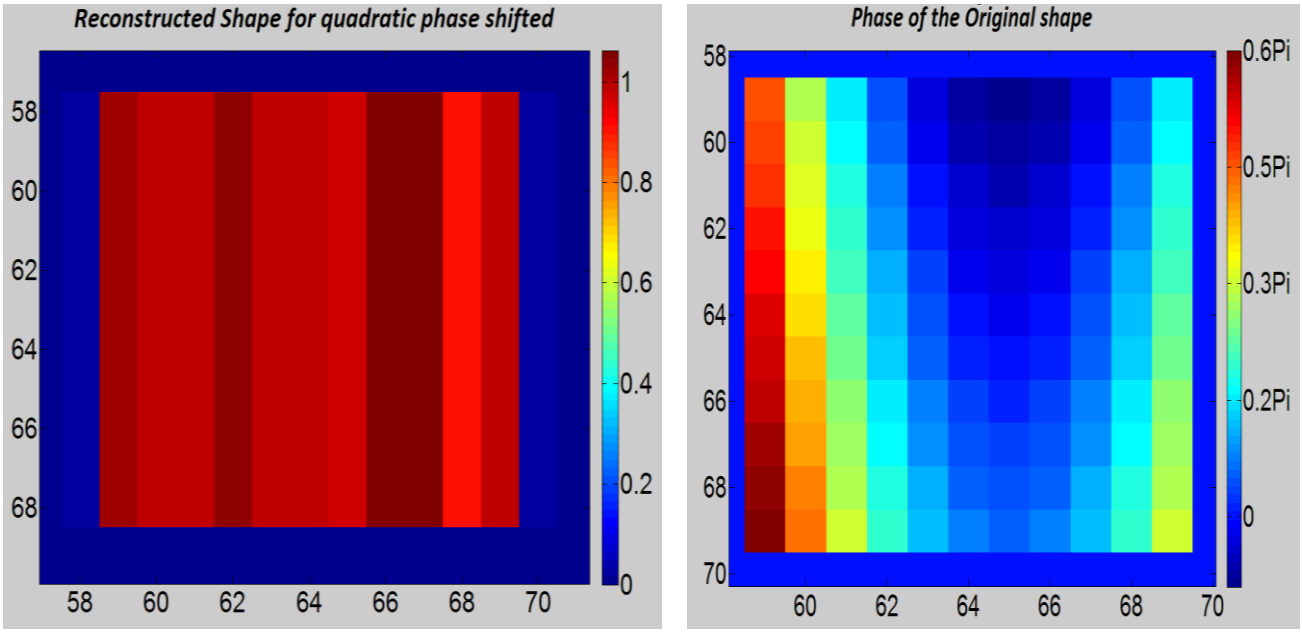

25%. Further shifting of the phase structure the reconstruction reverted to reproducing objects and phase structures similar to that of the symmetric phase. This may be due to strong phase wraps in the corner and side of the original phase structure.

***Figure 38*** – One reconstructed phase structure for the shifted quadratic phase.

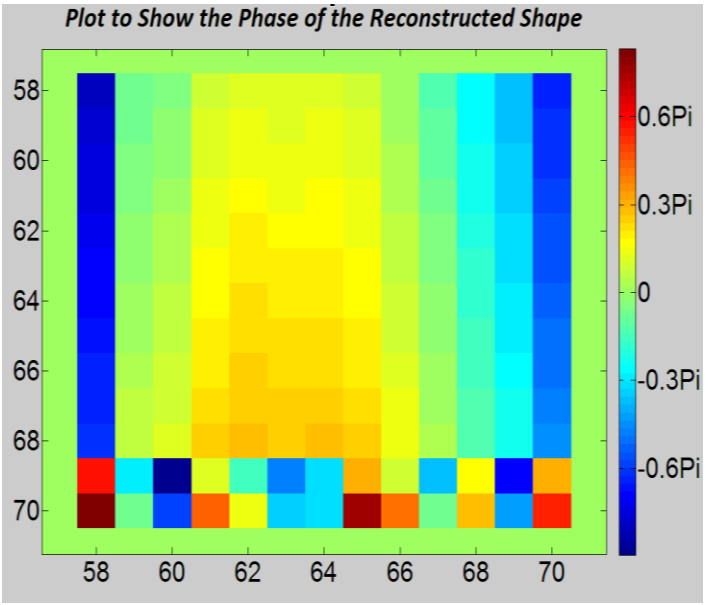


***Figure 39*** – The other reconstructed phase structure for the shifted quadratic phase.

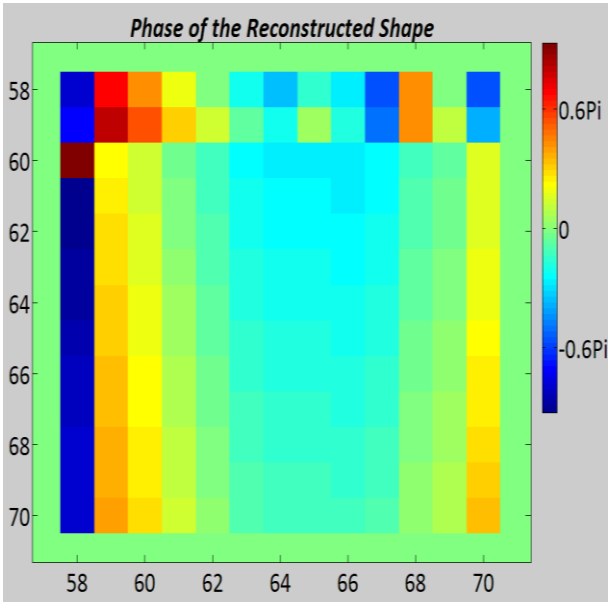


3.5 Effect of phase – saddle

A saddle point phase structure diffraction pattern is indistinguishable for four different phase structures:
Phase = $c1X^2 + c2Y^2$ An inward facing dome structure.
Phase = $-c1X^2 - c2Y^2$ An outward facing dome structure.
Phase = $-c1X^2 + c2Y^2$ A saddle point with a negative x quadratic and positive y quadratic
Phase = $c1X^2 - c2Y^2$ A saddle with a positive x quadratic and negative y quadratic
Examples of these phase structures are shown in figures 40 to 43. The expected result was that each

***Figure 40*** – Saddle structure phase: $-c1X^2 + c2Y^2$

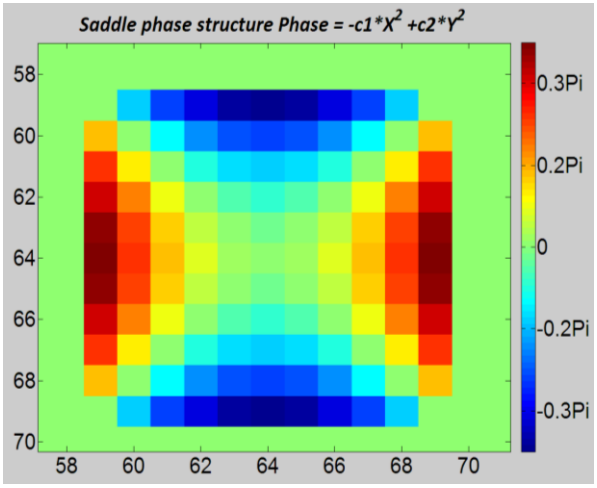


***Figure 41*** – Saddle structure phase: $c1X^2 - c2Y^2$

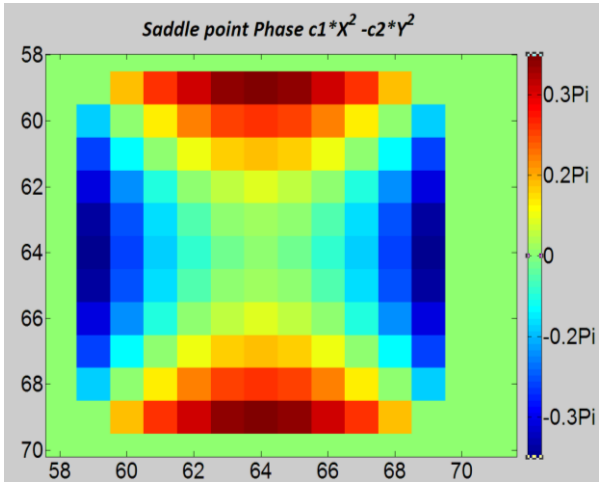

of the phase structures would be reconstructed 25% of the occasions.

***Figure 42*** – Outward facing dome phase: $-c1X^2 - c2Y^2$

***Figure 43*** – Outward facing dome phase: $c1X^2 + c2Y^2$

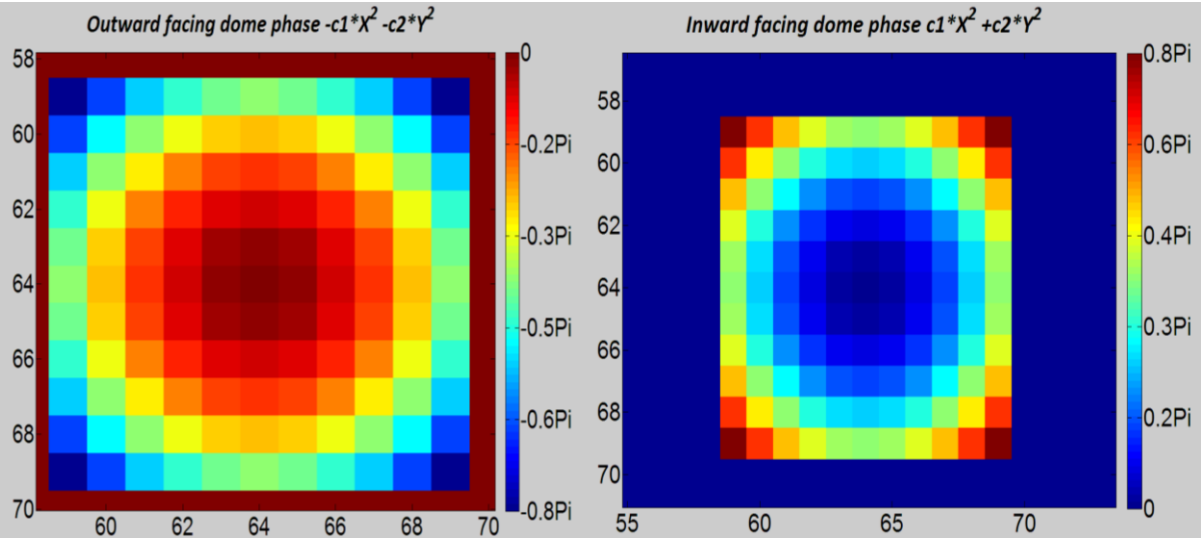


Figure 44 shows the associated diffraction pattern with figures 40 to 43. Again the fringes have started to become indistinguishable and blur together and the diffraction pattern has started to change to look more like a circular diffraction patter rather than the square pattern.

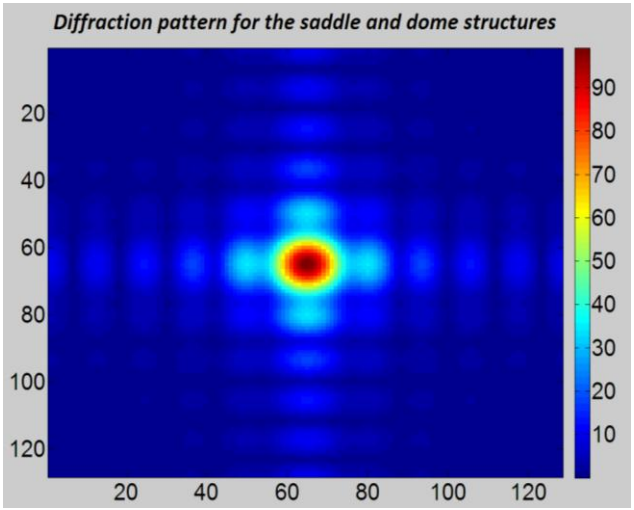


***Figure 44*** – The diffraction pattern associated with the four different phase structures: the inward facing dome, the outward facing dome, the saddle point with positive Y and negative X and the opposite saddle structure.

***Figure 45*** – Reconstruction of the inward facing dome reconstruction

***Figure 46*** – Reconstruction of the outward facing dome reconstruction

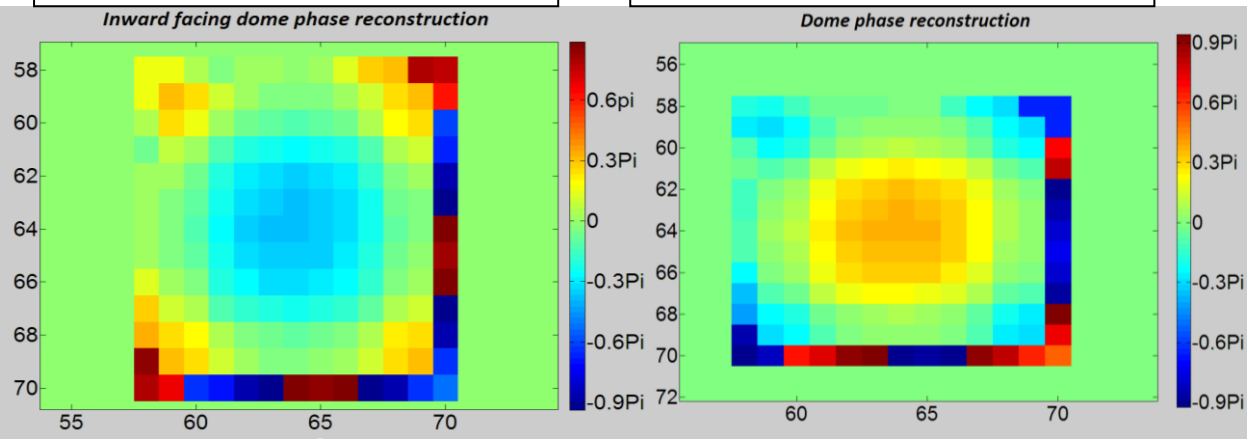


The phase occurrence is summarised in table 2. A percentage of no phase is present for this reconstruction an unexpected result that is most likely caused by the program not getting started and becoming stuck in a minimum at the start of the iterations and so not tending towards a phase structure. To test this, a small amount of phase was added to the initial trail solution, this gave the expected result of 25% occurrence for each phase structure. The other unexpected result was that the saddle structure was not reconstructed, instead linear horizontal and vertical structures were reproduced as shown in figures 48 and 49. This may be because the saddle structure has a phase

***Figure 48*** – Phase reconstruction linear horizontal phase

***Figure 49*** – Phase reconstruction linear vertical phase

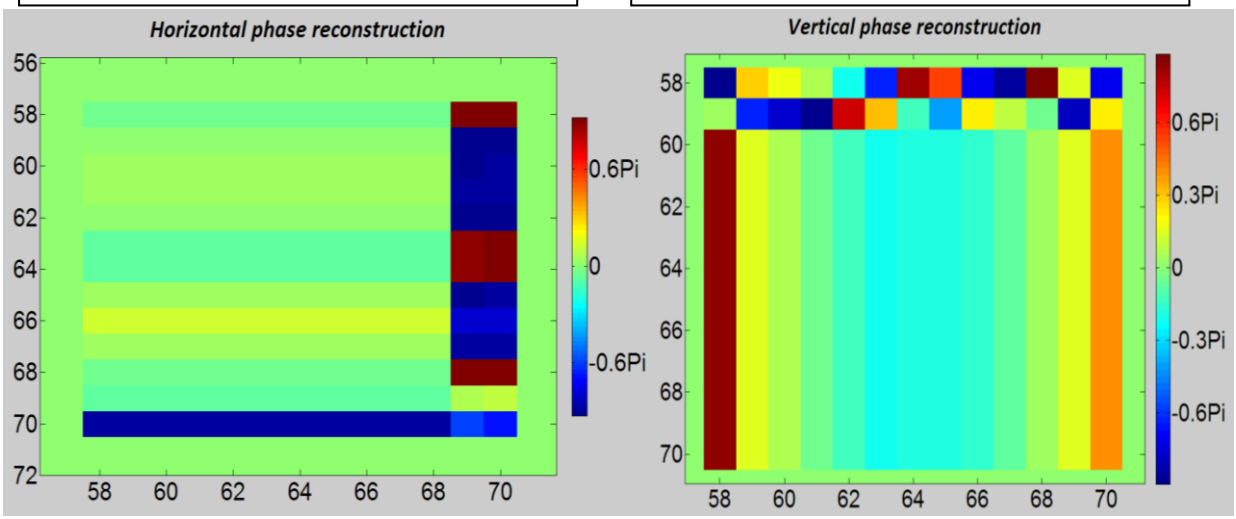


variation running through the shape from all four corners of the object leading to a local minimum structure of a linear structure. Whereas the dome shape phases only have a strong phase shift in very small areas at the corners of the object and so it is easier to reconstruct this type of structure.

**Table 2 – A table to show the occurrence of different phase structures for a symmetrical saddle point phase structure**

| **Phase** | $c1X^2 + c2Y^2$ | $-c1X^2 - c2Y^2$ | Linear Horizontal | Linear vertical | 0 Phase |
|---|---|---|---|---|---|
| **Occurrence %** | 27 | 22 | 22 | 16 | 13 |

3.6 Effect of phase – Saddle point shifted

Adding a shift to the saddle point structure in both the X and Y direction as shown in figure 51 had several effects like the shift in the quadratic phase. The diffraction pattern has shifted from the central position toward the bottom right hand corner of the matrix. This is different to the quadratic phase as the shift in the diffraction pattern is in the same direction as the saddle point shift. Adding the phase shift has the effect of reducing the phase variation allowing for reconstructions for object with up to π variation across them. The figures 50 to 60 have all been reconstructed with a phase of π across the object as weaker phase variation had subtler results that were harder to distinguish. Several phase structures were created that were not expected although the frequency so low they can only be counted as anomalies, the results are summarised in table 3 and the reconstruction appears to be biased towards the outward facing dome construction reconstructing this shape on 66% of all outcomes.

***Figure 50*** - The diffraction pattern of the shifted saddle point structure

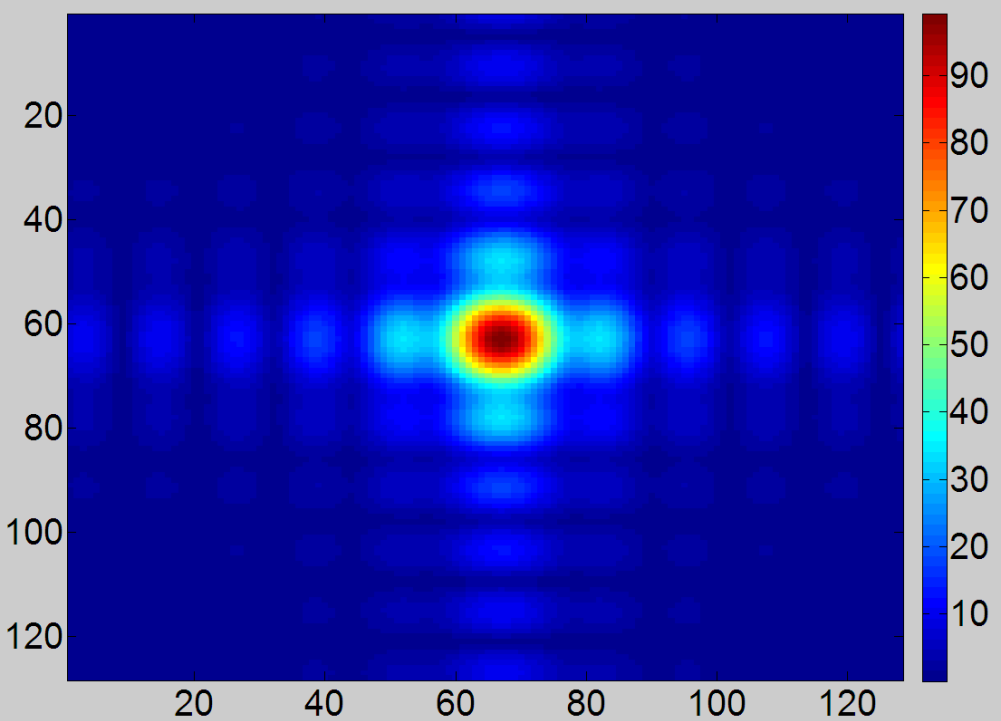

***Figure 51*** – The shifted saddle point structure of the original object

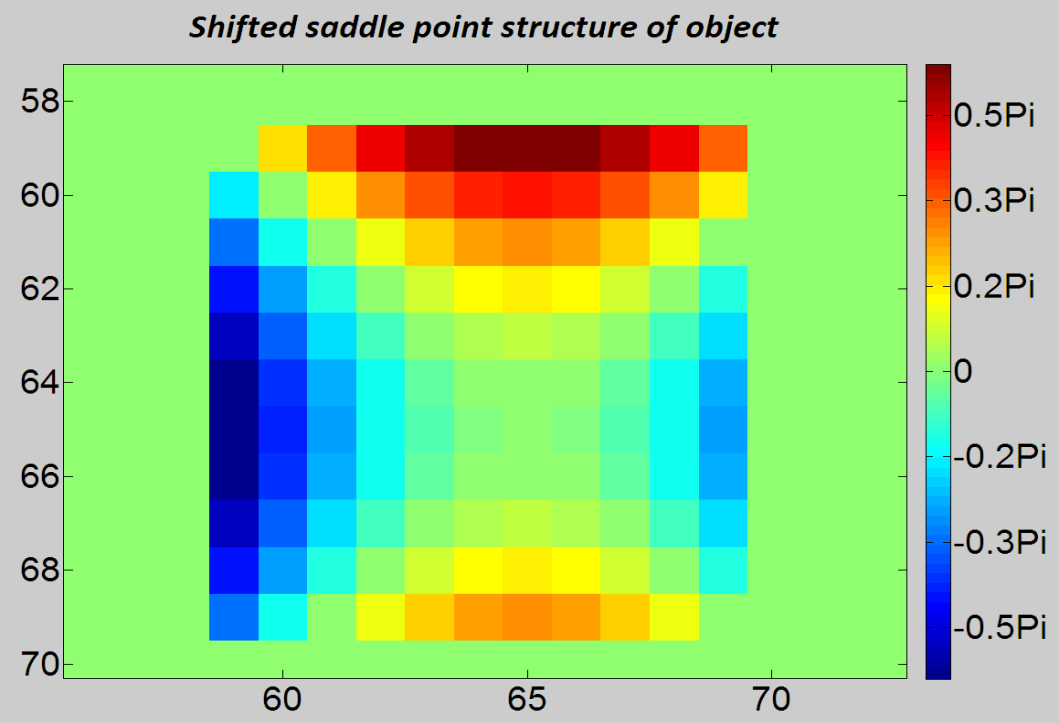


***Figure 52*** – The outward dome Phase reconstruction. This has been shifted towards the top right hand corner.

***Figure 53*** – The inward dome Phase reconstruction. This has been shifted towards the bottom left hand corner.

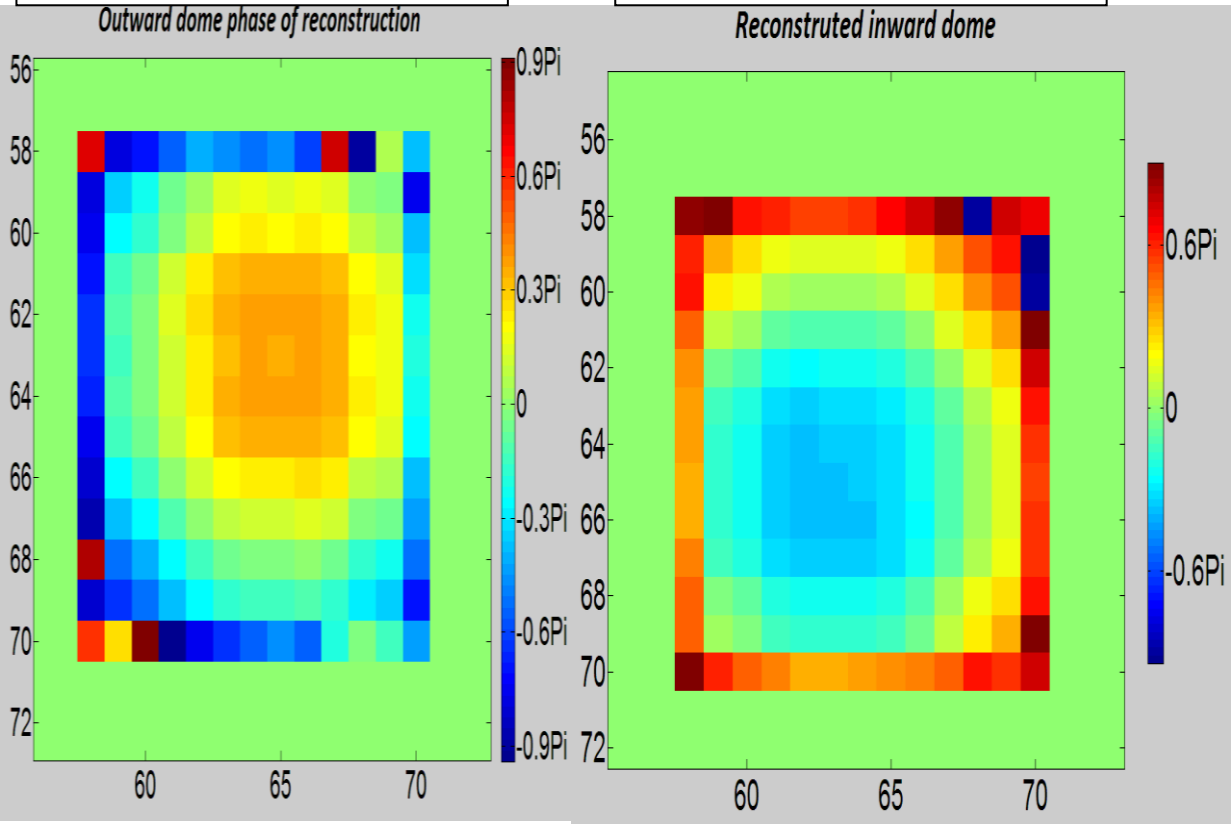

***Figure 54*** – This figure shows the phase reconstruction producing a negative quadratic in the Y direction. The scale is the same as figures 52 and 53.

***Figure 55*** – This figure shows the phase reconstruction producing a negative quadratic in the X direction. The scale is the same as figures 52 and 53.

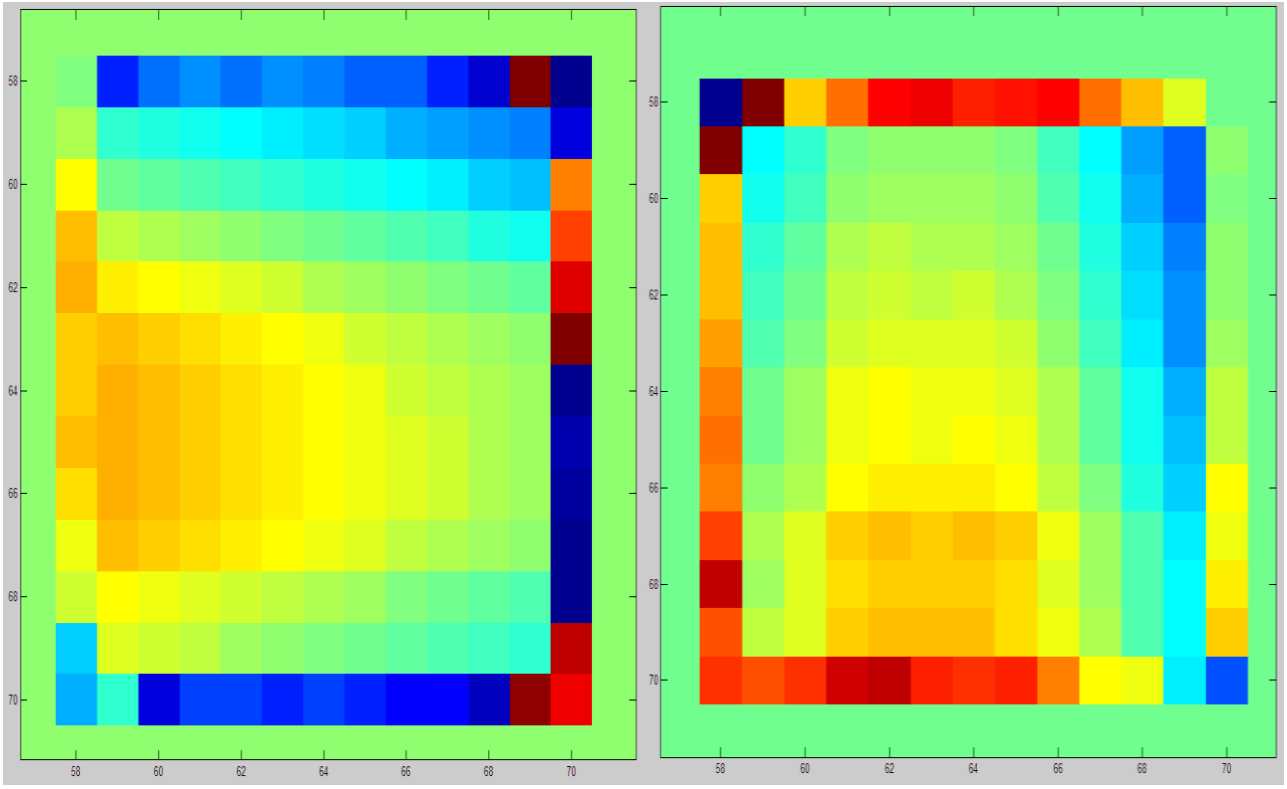


***Figure 56*** – This figure shows the phase reconstruction producing a positive quadratic in the Y direction. The scale is the same as figures 52 and 53.

***Figure 57*** – This figure shows the phase reconstruction producing a positive quadratic in the X direction. The scale is the same as figures 52 and 53.

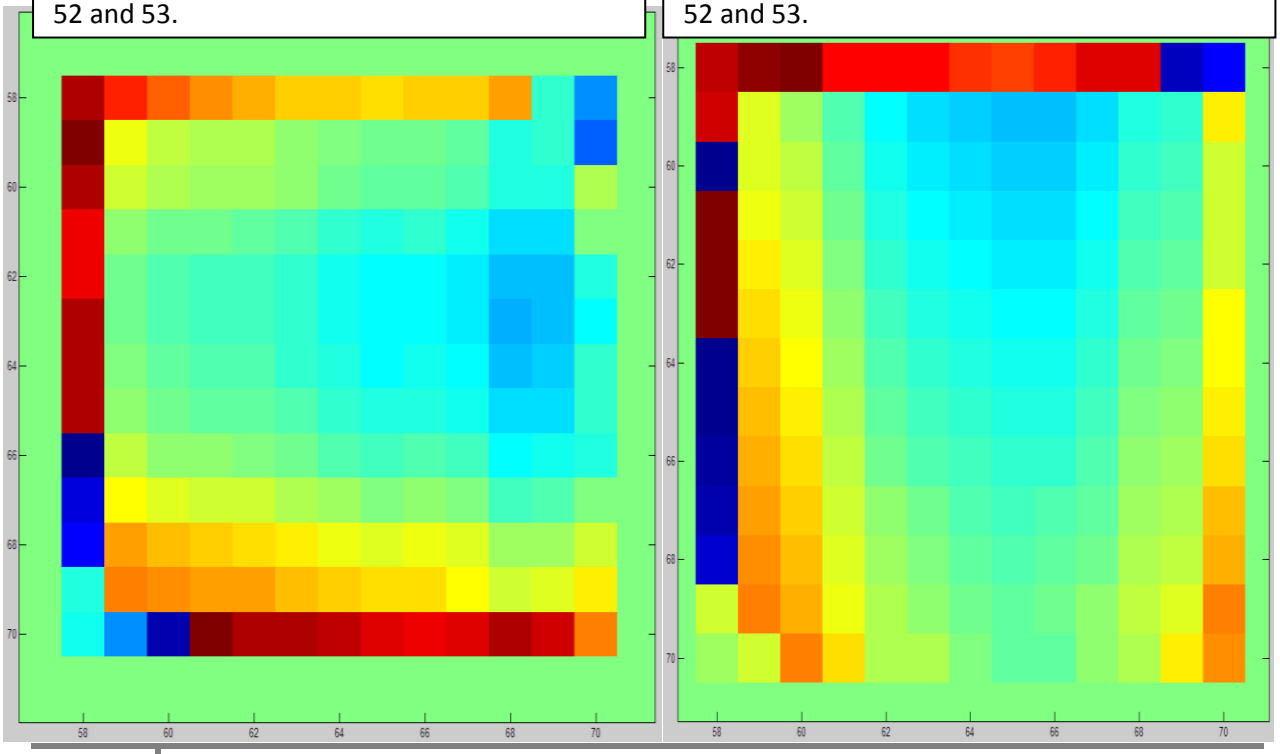

***Figure 58*** – A saddle point like phase reconstruction with positive Y direction and negative X direction. The scale is the same as figures 52 and 53.

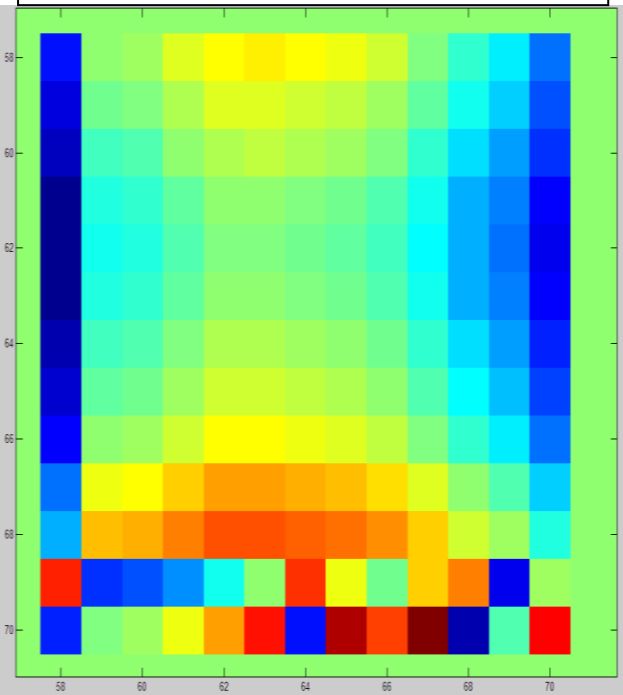


***Figure 59*** – A saddle point like phase reconstruction with positive X direction and negative Y direction. The scale is the same as figures 52 and 53.

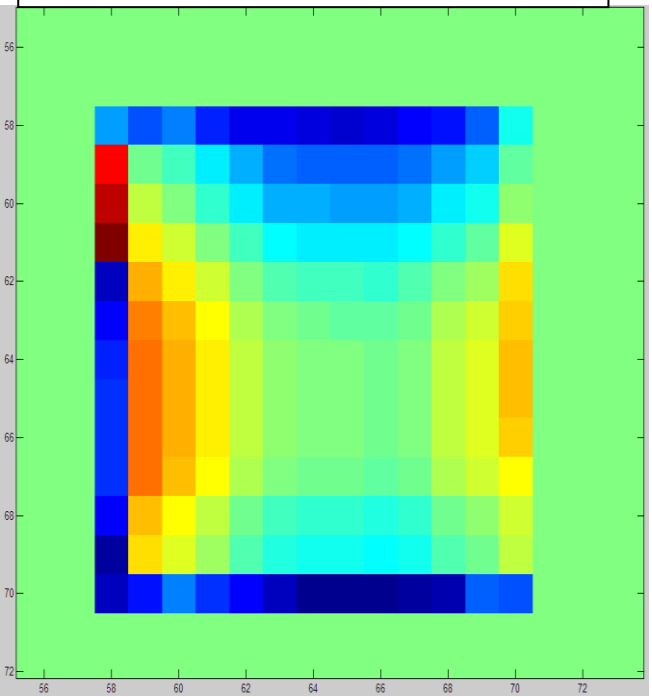


***Figure 60*** – A linear phase structure of phase: $2\pi Xc + 2\pi Yd$ where c and d are constants. The scale is the same as figures 52 and 53.

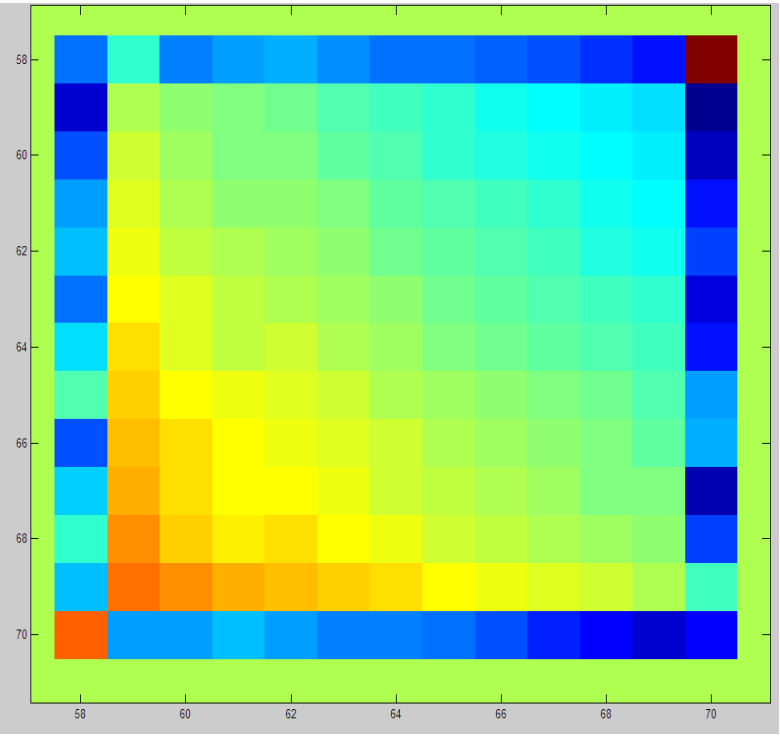

| Table 3 – A table to show the occurrence in % of the shifted saddle point phase structure | | | | | | |
|---|---|---|---|---|---|---|
| **Phase** | $-x^2 -y^2$ | $x^2 +y^2$ | $+y^2 -x$ | $-y^2 +x$ | $x^2 -y$ | $-x^2 +y$ |
| % | 61 | 22 | 3 | 2 | 3 | 6 |
| **Phase** | **Symmetrical** | $-x^2 +y^2$ **Saddle** | $x^2 -y^2$ **Saddle** | | | |
| % | <1 | <1 | <1 | | | |

The reconstruction was run over 200 separate occasions to compile these results. Both the saddle phases and the symmetrical phase structures only appeared on less than 1% of the occasions so their presence can be considered as anomalies. The quadratic phase structures that have been created also appear on a very small number of occasions. A likely reason as to why they are being constructed is that they are heavily shifted saddle points. In figure 54 to 57 the quadratic phase under goes a strong phase variation in one of the corners that looks very much like a saddle point structure. If these are saddle points the reconstruction is heavily biased against constructing these features. This may be because of the large regions of strong phase variation in saddle point structures the reconstruction program seems to only be able to reconstruct these large phase variations in the corners of the objects and biasing the inward facing dome and altering the saddle point phase reconstruction. Shifting the saddle point by another pixel in both the Y and X direction switches the bias to the outward facing dome structure reconstructing this on around 63% of all the occasions. The inward facing dome was recreated on around 23% of all the occasions and the quadratic phase structures again had very low percentage outcomes. Shifting the saddle point by 3 pixels gave a strong bias towards the symmetrical phase structure reconstruction appearing on 50% of the occasions. Saddle structures appeared on less than 1% of the occasions and the dome constructions appeared around 25% of the time each. The error for a 3-pixel shift was increased massively and the reconstruction no longer produced recognisable shapes so the program is only able to handle 2 pixel shifts before the phase variation needs to be lowered in order for recognisable shapes to be reproduced. Shifting the saddle in just the X or Y direction gave a heavy bias towards the quadratic phase structures, as this is similar to the phase structure. If shifted in the X direction Y quadratic structures of both the positive Y quadratic and the negative Y quadratic like figures 54 and 56. For shifts in the Y direction X quadratic structures were produced both positive and negative such as figure 55 and 57. Dome reconstructions, saddle points or linear reconstructions did not appear. So a shift in the X or Y direction means the phase is no longer recognised as a saddle point by the reconstruction and defaults to producing quadratic phase structures.

# 4. Improvements

It has been shown that for strong phase variation across objects the reconstruction breaks down as the reconstruction has numerous solutions interconnected by the propagation uniqueness problem. The support constraint, which works for weaker phase variation by finding the solution with the smallest dimensions, is no longer applicable because propagation for strong phase objects can make the object smaller and so the reconstruction would be finding the wrong solution. To solve this problem and reconstruct objects and images with strong phase variation real-space information about the object needs to be applied in order for the reconstruction program to reduce down to the desired solution. Two different methods of adding real space information are reviewed: Constraining the magnitude information of the trial solution studied by A. Minkevich (Minkevich, 2011) and constraining the phase information of the trial solution studied by X. Shi (Shi, unpublished).

4.1 Including magnitude information – Minkevich

The Minkevich method adds known information about the magnitude of the object, discussed in his papers as electron density, into another real space constraint. As well as using the weighted average support constraint applied in the HIO algorithm the magnitude of a large area of the trial solution is only allowed to vary in a very small magnitude range or set to a specific value. The edges of the object were not confined to the magnitude constraint as this area in the GaAs wires that was studied is subject to the most stress and so can change (Minkevich, 2011). This added constraint improves the stagnation of the HIO- ER algorithm technique and requires fewer iterations in order to successfully reconstruct the objects improving run times and memory consumption.

In section 3 of this report the effects of phase on the object reconstruction was investigated. A specific reconstructed magnitude was found for each of the phase structures associated with the shifted unsymmetrical phases. This was most noticeable for the shifted saddle point. An example of this is shown in figure 61, this specific magnitude structure was reproduced only for the phase structure shown and no other magnitude structures were produced for that phase structure. This linking between the phase and magnitude means that when a Minkevich magnitude constraint is applied the phase is also restricted to a certain structure. The constraint applied to both phase and magnitude would drive the

***Figure 61(a) and (b)*** - Figure (a) shows the magnitude structure that was reproduced every time when figure (b) phase structure was reconstructed. The magnitude varies here between 0.8 and 1.2.

(a) (b)

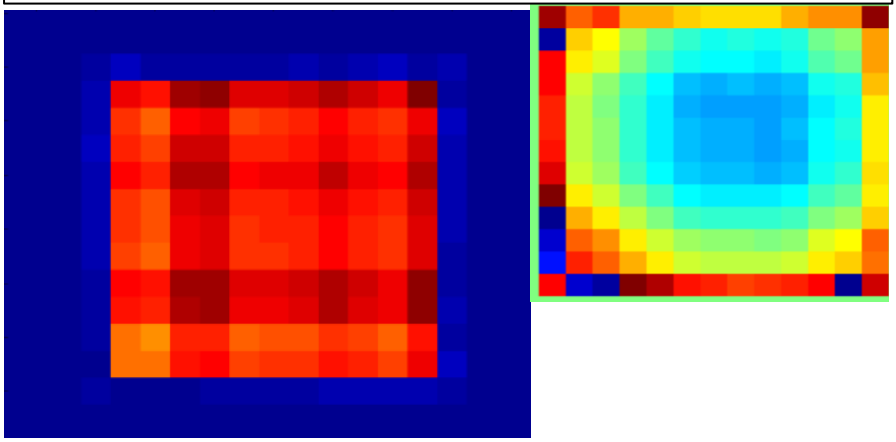

reconstruction very quickly to the correct solution and allow for large phase variation to be reconstructed within the centre of the object. For symmetrical phase objects the magnitude reproduced for each of the phases was the same so restricting the magnitude in this case might reconstruct the two different phase structures.

4.2 Including phase information – Shi

In many cases the magnitude information of the object is unknown. In certain cases the phase structure of the object can be approximated for example the stress and strain across wires. This leads to another way of adding a real space constraint. A phase structure for the constraint needs to be programmed and then the phase can be allowed to vary away from this structure by a certain amount. This is applied again at the same time as the sample space average weighting constraint in the HIO iteration process and the at the sample space constraint in the ER iteration process. This technique was found to work very well when the phase variation around the structure was less than 0.5π.

As the phase structure and magnitude information appear to be linked this would be a very successful method of reconstructing the object as for symmetrical phased objects the correct magnitude could also be found.

The potential of the Shi model was tested in this program by adding the known phase structure to the initial trial solution. As long as it was within a very close range of around 0.1 to 0.2 π this initial trial solution guided the reconstruction successfully towards the correct reconstruction for stronger phase variation across the programmed objects.

# 5. Conclusion

The project set out to construct a program to reconstruct objects from their diffraction patterns and to investigate how adding phase affected the reconstruction. The program build was very reliable for objects with no phase. It did not require much computational effort or time and was not dependent on the initial trial solution. Adding small amounts of phase variation less than or equal to 0.5 π the program was again reliable and efficient at reconstructing these objects and their phase structures. A linear shift corresponded to a translation of the diffraction pattern which when removed would reconstruct the object successfully for even strong phase. Quadratic phase structure was more difficult for the program to reconstruct and the phase variation needed to be lowered to 0.1π up to 0.2π for the program to be considered reliable in its reconstruction. Shifting the quadratic phase in the X direction made the phase structure more manageable for the program and phase variation up to 0.5π could be done. This also seemed to bias the reconstruction toward a particular phase structure type where as equal amounts of the possible phase structures was expected. For the saddle point type structure, the phase variation had to be lowered to around 0.2π for the reconstruction to be reliable. Four phase structures were expected with five (no of which was no phase) being produced. By introducing a small amount of phase into the initial guess the 0 phase structure was no longer produced but the program still was not able to produce the saddle structures expected only linear type phase structures. Shifting the saddle point in both the X and Y

direction added a bias towards the inward facing dome reproducing this around 61% of the occasions. The saddle point type structures were still not produced instead quadratic phase structures were created but only around 15% of the time. I believe the algorithm cannot reconstruct small areas of strong phase changes which bias the smoother dome type phase and why the program cannot reconstruct saddle point type structures.

To improve and extend the reconstruction program so that stronger phase variation can be reconstructed, more real space information needs to be known and imposed within the program. Two different techniques of doing this is the magnitude constraint method developed by Minkevich or the phase constraint method developed by Shi. The diffraction pattern for certain phase structures is the same. So the phase constraint method has a lot of potential as it removes this uncertainty. Finding the approximate phase structure of an object may be difficult though where as a magnitude constraint could be programmed using information from the diffraction pattern and optimised through an iterative process before being used in the reconstruction.

To conclude, adding phase structures to objects alters the diffraction pattern and makes the reconstruction more difficult due to the propagation uniqueness problem. In order to reconstruct these objects real space information needs to be applied in order for the reconstruction process to create the desired object. Shifting symmetrical phase structures imposes a bias towards a particular phase structure that could possibly be due to small areas of strong phase variation in the object being difficult for the program to reconstruct.

## 6. References

Bauschke, H. H. Combettes, P. L. and Luke, D .L. (2002) 'On the Structure of Some Phase Retrieval Algorithms' *Image Processing 2002,* vol 2, *IEEE Xplore Digital library* [Online] Available at: http://ieeexplore.ieee.org/xpl/login.jsp?tp=&arnumber=1040082&url=http%3A%2F%2Fieeexplore.ieee.org%2Fxpls%2Fabs_all.jsp%3Farnumber%3D1040082 (Accessed: 10 January 2013).

Cha, W. Song, S. Jeong, N. C. Harder, R. Yoon, K. B. Robinson, I. K and Kim, H. (2010) 'Exploration of Crystal Strains Using Coherent X-ray Diffraction' *New Journal of Physics, IOP Science* [Online] Available at: http://www.opticsinfobase.org/oe/abstract.cfm?uri=oe-20-15-17093 (Accessed: 10 January 2013).

Clark, J. N. Huang, X. Harder, R and Robinson, I. K. (2012) 'High-Resolution three-dimensional Partially Coherent Diffraction Imaging' *Nature Communications, 3:99, Nature* [Online] Available at: http://www.nature.com/ncomms/journal/v3/n8/full/ncomms1994.html (Accessed: 10 January 2013)

Goodman, J.W. (2005) *Introduction to Fourier Optics* 3rd edn. Robert and Company Publishers

Huang, X. Harder, R. Xiong, G. Shi, X and Robinson, I. (2011) 'Propagation Uniqueness in Coherent Diffractive Imaging' *Physics Review B,* vol 83, *American physical Society* [Online] Available at: http:// http://prb.aps.org/abstract/PRB/v83/i22/e224109 (Accessed: 10 January 2013)

KÖhl, M. Minkevich, A. A and Baumbach, T. (2012) 'Improved Success Rate and Stability for Phase Retrieval by Including Randomized Overrelaxation in the Hybrid Input Output Algorithm' *Optics Express,* Vol 20, issue 15, Optics Info Base OSA's Digital Library [Online] Available at: http://jpsj.ipap.jp/journal/JPSJ-82-2.html (Accessed: 8 February 2013).

Marchesini, S. He. H. Chapman, H.N. Hau-Riege, S.P. Noy, A. Howells, M. R. Weierstall, U and Spence, H. (2003)'X-ray image reconstruction from a diffraction pattern alone' *Physical Review B,* **68,** 140101, *American Physical Society* [Online] Available at: http://prb.aps.org/abstract/PRB/v68/i14/e140101 (Accessed: 8 February 2013).

Miao, J. and Sayre, D. (2000)'On Possible Extensions of X-ray Crystallography through Diffraction-Pattern Oversampling'. *Acta Crystallogr. A* 56, 596–605, *Foundations of Crystallography* [Online] Available at: http://www.physics.ucla.edu/research/imaging/Publications/pdf/ac_2000_a56.pdf (Accessed: 8 February 2013).

Miguel, A. Aranda, G. Berenguer, F. Bean, R. J. Shi, X. Xiong, G. Collins, S. P. Nave, C and Robinson, I. 'Coherent X-ray Diffraction Investigation of Twinned Microcrocrystals' *journal of Synchrotron Radiation,* 17, 751-760, EJC Search [Online] Available at: http://journals.ohiolink.edu/ejc/search.cgi?q=authorExact:%22Shi%2C%20Xiaowen%22 (Accessed: 8 February 2013).

Minkevich, A. A. Fohtung, E. Slobodskyy, T. Riotte, M. Grigoriev, D. Metzger, T. Irvine, A. C. Novak, V. Holy, V and Baumbach, T. (2011) 'Strain Field in (GA,Mn)AS/ GaAs Periodic Wires Revealed by Coherent X-ray Diffraction' *A Letters Journal Exploring the Frontiers of Physics, 94, EPL Journal* [Online] Available at: http://iopscience.iop.org/0295-5075/94/6/66001 (Accessed: 8 December 2012).

Robinson, I. K and Harder, R. (2009) 'Coherent X-ray Diffraction Imaging of Strain at the Nanoscale' *Insight Review Articles, vol 8, Nature Materials* [Online] Available at: http://www.im2np.fr/news/presse/Nature_Robinson_2009_IM2NP.pdf (Accessed: 8 December 2012).

Robinson, I. (2012) 'Nanoparticle Structure by Coherent X-ray Diffraction' *Journal of the Physical Society of Japan,* Vol 82. [Online] Available at: http://jpsj.ipap.jp/journal/JPSJ-82-2.html (Accessed: 8 February 2013).

Shi, X. (2012). Unpublished PhD thesis. University College London

Vartanyants, I. A., Pitney, J. A., Libbert, J. L. and Robinson, I. K.(1997) 'Reconstruction of surface morphology from coherent X-ray reflectivity'. *Physical Review B* **55,** 13193–13202*, American Physical Society* [Online] Available at: http://prb.aps.org/abstract/PRB/v55/i19/p13193_1 (Accessed: 8 February 2013).

Williams, G. J., Pfeifer, M. A., Vartanyants, I. A. and Robinson, I. K. (2007) 'Effectiveness of iterative algorithms in recovering phase in the presence of noise' Acta Crystallographica Section A Foundations of Crystallography Volume 63, Part 1. *A* 63, 36–42 *Foundations of Crystallography*

[Online] Available at: http://journals.iucr.org/a/issues/2007/01/00/issconts.html (Accessed: 8 February 2013).

# 7. Appendix

7.1 ER Program

```
function [newshape Phaseshape]= nophasesquare()
alpha = 100000;%defining the number of iterations for the first ER
ny=128;%defining pixels space lines 6&7
nx=128;
ax=55;%defining sample space dimensions lines 8&9
ay=73;
    function [Phaseshape] = Oshape(nx,ny)%creating the original shape
A= zeros(ny,nx);
 A(59:69,59:69)=1;
Phaseshape=A;
    end
Phaseshape=Oshape(nx,ny);
figure;% Plotting images of the original shape
imagesc (angle(Phaseshape));
title ('Figure 1 - Plot to Show the Phase of the Original shape');
colorbar;
figure;
imagesc (abs(Phaseshape));
title ('Figure 2 - Plot to Show the Magnitude of the Original shape');
colorbar;

    function ss= samplespace(nx,ny,ax,ay)% creating an M file for random
guess
ss=zeros(ny,nx); %creating a random guess of original shape 'sample space'
    ss(ax:ay,ax:ay)=rand(1);
    end

ss=samplespace (nx,ny,ax,ay);%first random guess

figure;%Images of the random guess
imagesc (angle(ss));
title ('Figure 3 - Plot to Show the Phase of the First Guess');
colorbar;
figure;
imagesc (abs(ss));
title ('Figure 4 - Plot to Show the Magnitude of the First Guess');
colorbar;

    function [recondata, errorER] = ER(Phaseshape,ss,nx,ny,ax,ay)% creating
an M file for reconstructing the phase ER1
    fftshape=fft2(fftshift(Phaseshape));% Fourier transformation of
original shape
    fftShape=fftshift(fftshape);% shift DC component of Fourier transform
to centre of spectrum
```

```
    data =abs(fftShape);%representation of 'collected data'
    B= zeros(ny,nx);%constructing the sample constraint again
    B(ax:ay,ax:ay)=1;
        for l= 1:alpha
        ffta=fft2(fftshift(ss));% Fourier transformation of sample space
        fftA=fftshift(ffta);% shift DC component of Fourier transform to
centre of spectrum
        phase=angle(fftA);% keeping the phase information
        magnitude=abs(data);%using the magnitude information of the 'data'
        fftB= magnitude.*exp(1i* phase); % combining to form a new matrix

        fftb=fftshift(fftB); % shifting the DC component back to the coners
before inverse transformation
        b=fftshift(ifft2(fftb));% result

        recondata = B.*b;% applying the sample constraint again
        ss=recondata;
            errorER(l)=chisquared(data,fftA); % error calculation
            errorER(l)
        end
    end
recondata = ER(Phaseshape,ss,nx,ny,ax,ay);
figure;%Images of the reconstructed shape
imagesc (angle(recondata));
title ('Figure 5 - Plot to Show the Phase of the Reconstructed Image 4
Pixels larger after 100000 Iterations');
colorbar;
figure;
imagesc (abs(recondata));
title ('Figure 6 - Plot to Show the Magnitude of the Reconstructed Image 4
Pixels larger after 100000 Iterations');
colorbar;
end
```

7.2 HIO Program

```
function [d]= HIO (Phaseshape, c,nx,ny,ax,ay)%Creating an M file
    beta=0.9;

    fftshape=fft2(fftshift(Phaseshape));% Fourier transformation of
original shape
    fftShape=fftshift(fftshape);% shift DC component of Fourier transform
to centre of spectrum
    data =abs(fftShape);%representation of 'collected data'

     B= zeros(ny,nx);%constructing the sample constraint again
    B(ax:ay,ax:ay)=1;

        for l= 1:delta

        ffta=fft2(fftshift(c));% Fourier transformation of sample space
        fftA=fftshift(ffta);% shift DC component of Fourier transform to
centre of spectrum
```

```
        phase=angle(fftA);% keeping the phase information
        magnitude=abs(data);%using the magnitude information of the 'data'
        fftB= magnitude.*exp(i* phase); % combining to form a new matrix

        fftb=fftshift(fftB); % shifting the DC component back to the
corners before inverse transformation

        b=fftshift(ifft2(fftb));% result

        d = (b.*B)+(1-B).*(c-beta*b);
        c=d;
        errorER(l)=chisquared(data,fftA);
            errorER(l)

        end
    end
```

7.3 Phase construction Program

```
function [Phaseshape] = Oshape (nx,ny)
A= zeros(ny,nx);
 A(59:69,59:69)=1;
[X,Y]=meshgrid(0:(nx-1),0:(ny-1));% mesh grid created to turn matrix into
vectors
X=X-nx/2;
Y=Y-ny/2;
phase=exp(i*cpi*pi*(c1*(X+c2).^2+c3+c4*Y.^c5));
```